

Cryogenic Carbon Capture of a Cement Plant Off-gas considering the Synergies of a PtX Integration

A technical and optimisation study of cryogenic
solid-vapour separation

Frede Malthe Lindquist, Kristoffer Holst

Energy Engineering, TEPE4-101, 2022-05

Master's Thesis





AALBORG UNIVERSITY
STUDENT REPORT

Energy Technology
Aalborg University
<http://www.aau.dk>

Title:

Cryogenic Carbon Capture of a Cement Plant Off-gas considering the Synergies of a PtX Integration

Theme:

Master's Thesis

Project Period:

Spring Semester 2022

Project Group:

TEPE4-1001

Participant(s):

Frede Malthe Lindquist
Kristoffer Holst

Supervisor(s):

Thomas Helmer Pedersen
Daniele Castello

Page Numbers: 92

Date of Completion:

May 28, 2022

Abstract:

The Cryogenic Carbon Capture process can decrease the energy demand for CO₂ separation and pressurisation to 150 bar significantly, compared to other conventional technologies. The CCC process is a post-combustion technology that utilises cryogenic conditions to separate CO₂ from the other contaminants in the cement plant off-gas. The energy duty for the CCC process is estimated both with the use of an empirical off-gas composition and a modelled off-gas composition. The modelled calcination and combustion process is based on a methane fired combustion and a calcination process with a pure CaCO₃ supply. Furthermore, the CCC process is benchmarked to the theoretical minimum energy duty for CO₂ separation to consider the potential for further improvements. It appears that the CCC technology's high potential for heat integration is crucial in order to achieve a competitive energy duty. Furthermore, based on the sensitivity study, it appears that the most dominating parameter affecting the energy duty is the CO₂ concentration in the off-gas. Moreover, the synergies between the calcination and combustion process, the CCC process, and a Power to X facility are investigated to explore the possibility of converting the captured CO₂ into methane, which can be utilised to force the calcination reaction and make a self-supplying process.

The content of this report is freely available, but publication (with reference) may only be pursued due to agreement with the author.

By accepting the request from the fellow student who uploads the study group's project report in Digital Exam System, you confirm that all group members have participated in the project work, and thereby all members are collectively liable for the contents of the report. Furthermore, all group members confirm that the report does not include plagiarism.

Summary

Carbon Capture, Utilisation and Storage (CCUS) technologies have recently received increased interest in order to decrease the CO₂ emission. In Denmark, Aalborg Portland is the single largest CO₂ emitter and constitutes 4 % of the national CO₂ emission. Furthermore, the introduction of new CO₂ emissions quotas and emission taxes will result in a cost of 1.86 billion DKK/year for Aalborg Portland unless a carbon capture solution is retrofitted. Thus, the incentive to find the most suitable carbon capture technology for Aalborg Portland is obvious.

This study aims to investigate the technical potential of cryogenic carbon capture (CCC) for separating CO₂ from the cement plant off-gas. The CO₂ separation is based on cryogenic solid-vapour separation, which utilises desublimation to remove CO₂ from the remaining contaminants. The cement plant off-gas scale and composition are initially approximated with data provided by Kær (2019). Based on the composition and flow specifications inspired by Kær (2019), the developed CCC process model could obtain a CO₂ purity of 99.96 mol.% with a corresponding CO₂ recovery of 99.9 %. By further optimising the CCC process with respect to the energy consumption and subsequently considering the potential of heat integration, a resulting energy duty of 0.89 MJ/kg of captured CO₂ can be achieved. Moreover, a sensitivity study of the CCC model with respect to the CO₂ off-gas concentration is conducted. The study showed that an increased CO₂ concentration results in a lowering in the energy duty. Consequently, the calcination and combustion process is modelled in order to investigate the potential to increase the CO₂ concentration. The calcination and combustion process is modelled based on a constant temperature and pressure of 1,500 °C and 1 atm, respectively. The calcination process is modelled based on the CaCO₃ consumption at Aalborg Portland, and the associated combustion process is scaled based on the lower heating value of methane and the enthalpy of reaction. The combustion process is assumed to be methane fired, which can be produced in a methanation process. The methanation process utilises the captured CO₂ from the CCC process and hydrogen produced by an electrolysis process. The modelled calcination and combustion

process showed the possibility of increasing the CO₂ concentration in the off-gas by increasing the oxygen content in the oxidiser. However, the resulting adiabatic flame temperature of the oxyfuel combustion entails complications both in terms of the heat tolerance of the equipment and the thermal CO and NO_x formation. Conclusively, oxyfuel combustion is not recommended unless these complications are resolved. As a result, the oxidiser is solely air supplied, which leads to a direct air capture ability. By considering the CO₂ content in the air for the combustion process, the captured CO₂ will increase by 2,507 tonne/year. As the annual leak of CO₂ from the CCC process only amounts to 11 tonne/year, due to the high CO₂ recovery, the cement production in combination with a CCC technology can be considered CO₂ negative. In addition, the associated energy duty of the CCC process will be slightly reduced to 0.849 MJ/kg of captured CO₂, which results in an overall decrease in the energy consumption. The methane fired combustion process showed the possibility of increasing the off-gas CO₂ concentration resulting in a lowered energy duty for the CCC process. In Figure 1, the resulting energy duties for the CCC process are benchmarked to an empirical determined CCC process and several conventional carbon capture technologies. The CCC model* represents the energy duty associated with the off-gas discharged from the methane fired combustion and calcination process.

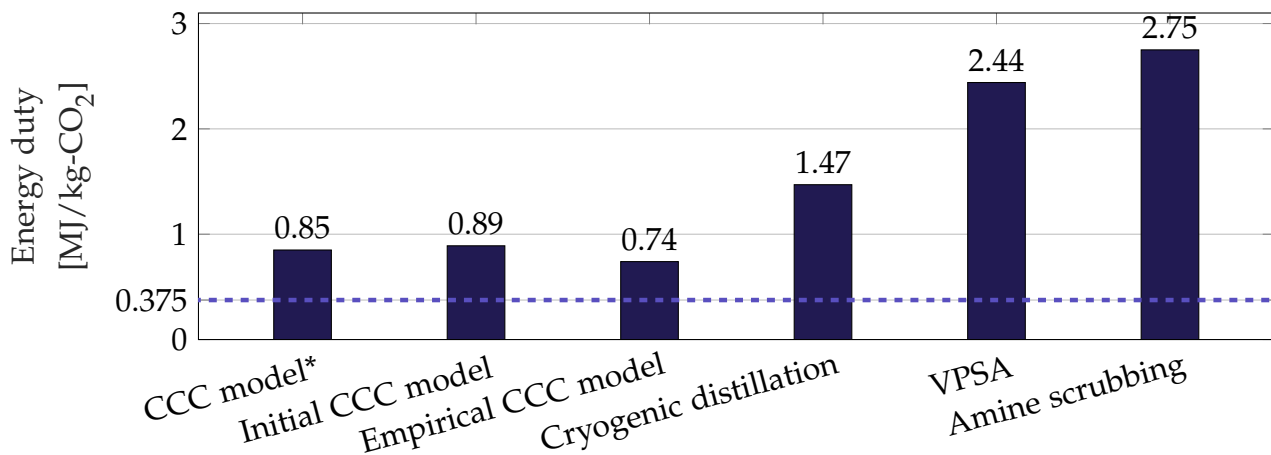


Figure 1: Comparison of the energy duties between the two developed CCC models and conventional carbon capture technologies

The CCC model* is based on an off-gas from the calcination process with a methane fired combustion. In addition, the - - - represents the theoretical minimum energy duty of 0.375 MJ/kg-CO₂ for CO₂ separation.

Conclusively, this study indicates that the CCC process is significantly less energy-consuming per kg of captured CO₂ compared to the conventional technologies. Furthermore, it appears that the energy consumption of the electrolysis and methanation processes is significantly higher than the CCC process. As a result, an economic evaluation must determine whether a PtX integration is a profitable solution. Subsequently, the economic evaluation must likewise determine whether a partial or entire methane conversion is the most profitable solution by evaluating the income of excess methane compared to disposal expenses for the CO₂ to storage.

Preface

The following master's thesis has been written by a pair of students on the 10th semester of Thermal Energy and Process Engineering at Aalborg University. Throughout this report, Aspen Plus[®], Cantera, and MATLAB[®] are used for modelling. The citation in this report is done by the use of the Harvard method (Author(s), Year) corresponding to the reference in the bibliography. All chapters and sections are provided with numbers presented in the table of contents. Figures, tables and equations have increasing numbers within each chapter. The authors would like to acknowledge Larry L. Baxter and Thomas Condra for their assistance.



Frede Malthe Lindquist
<flindq17@student.aau.dk>



Kristoffer Holst
<kholst17@student.aau.dk>

Nomenclature

Symbol	Quantity	Unit
c	Constraint	-
H	Enthalpy	$\frac{\text{kJ}}{\text{kg}}$
LHV	Lower Heating Value	kJ/kg
m	Mass	kg
Obj	Objective function	-
Q	Heat	kW
y	Mole fraction	-

Greek symbols:

Symbol	Quantity	Unit
η	Efficiency	-
λ	Excess air coefficient	-

Subscripts:

Symbol	Description
cal	Calcination
cond	Condenser
Desub	Desublimation
dry	Dryer
HEX	Heat exchanger
Melt	Melter
prod	Product
reac	Reactants
reboil	Reboiler

tot Total

Notation:

Symbol

Description

\dot{x}

Flow rate of x

s^{-1}

x^0

Standard of x

Chemistry:

Symbol

Description

$CaCO_3$

Limestone

CaO

Calcium Oxide

Ca^{2+}

Calcium-ion

CH_3OH

Methanol

CH_4

Methane

CO_2

Carbon dioxide

CO

Carbon monoxide

H_2O

Water

H_2

Hydrogen

HCl

Hydrochloric acid

HCO_3^-

Bicarbonate

N_2

Nitrogen

NO_x

Nitrogen oxides

O_2

Oxygen

SO_2

Sulphur dioxide

SO_x

Sulphur oxides

Abbreviation:

Description

AFR

Air to Fuel Ratio

APEA

Aspen Process Economic Analyser

CCS

Carbon Capture and Storage

CCU

Carbon Capture and Utilisation

CCUS

Carbon Capture, Utilisation and Storage

DAC

Direct Air Capture

EAC

Equivalent Annual Cost

IEA	International Energy Agency
PENG-ROB	Peng-Robinson
ppb	Parts per billion
ppm	Parts per million
PtX	Power to X
RWGS	Revers Water Gas Shift
TRL	Technology Readiness Level
VPSA	Vacuum Pressure Swing Adsorption

Contents

Preface	ix
Nomenclature	xi
1 Introduction	1
2 Problem Analysis	5
2.1 Introduction to CCUS	5
2.2 Cement Production Process	9
2.3 CO ₂ Purity Requirements for Electrofuel Production	13
2.4 Post-combustion CO ₂ Capture Technologies	15
2.5 Evaluation of the Separation Methods	23
3 Thesis Statement	27
3.1 Scope of the Project	27
4 Technical Analysis of the CCC Model	29
4.1 Scale and Composition	30
4.2 Cryogenic Carbon Capture Model	31
4.3 Optimisation of the CCC Model	40
4.4 Heat Integration	44
4.5 Sensitivity Analysis of the CCC Model	47
5 Technical Analysis of the Calcination and Combustion Process	49
5.1 Development of the Calcination and Combustion Model	49

5.2	Sensitivity Analysis of the Combustion Process	55
6	Integration to Power to X Chain	61
7	Evaluation of the Process Train	65
7.1	Direct Air Capture Ability	69
8	Conclusion	71
8.1	Recommendations for Future Studies	75
	References	77
A	Sub-Blocks in CCC Model	85
A.1	Dryer Component	85
A.2	Contact Liquid Coolant Circuit	86
B	Mass Flow Calculation of the combustion and utilisation processes	89
B.1	Specification of the Mass Flows for the Combustion Process	89
B.2	Scaling Specifications for the Utilisation Facility and the Electrolysis Process	91

Chapter 1

Introduction

The United Nations have adopted a sustainable development plan including 17 world goals. The 13th world goal is to take urgent action to combat climate change and its impacts (United Nations, 2016). Thus, the incentive for developing new sustainable technologies to lower greenhouse gas emissions is evident. The majority of the global CO₂ emission comes from the heat, electricity, transport, and heavy industry, where the heavy industry includes steel, iron, and cement production (Ritchie and Rosr, 2020), (Energistyrelsen, 2021). In the recent decades, the global cement production has experienced an increase, as presented in Figure 1.1. Due to the increasing cement production and the fact that it accounts for 7-10 % of global CO₂ emission, and 4 % of the Danish CO₂ emission, the cement industry constitutes a huge potential for Carbon Capture, Utilisation and Storage (CCUS) (Benhelal et al., 2021; Gardarsdottir et al., 2019; COWI, 2020). Despite the huge potential, none of the 45 large-scale CCUS projects in design, construction, or operation currently involves the cement industry (Hills et al., 2016). Consequently, it is crucial that the carbon capture technologies can be retrofitted to existing cement plants, to ensure that the cement plants do not need to be redesigned, which in the end minimises the complexity for the sustainable implementation.

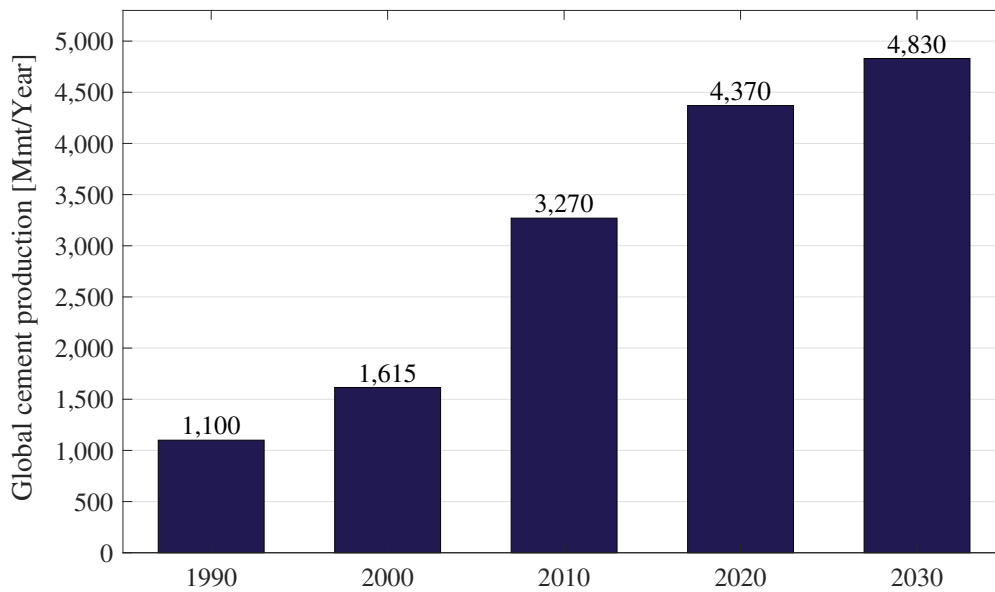


Figure 1.1: Global cement production per decade in million metric tons with data acquired from (Statista, 2020).

Unlike most industrial processes, process chemistry is the governing CO_2 emitter responsible for approximately 50 % of the total CO_2 emission (Farfan et al., 2019). This means that an implementation of CO_2 free fuels is not sufficient to eliminate the CO_2 emission from the cement production. In addition, it also means that a pre-combustion process is not sufficient, as this process solely captures the CO_2 from the combustion process. Consequently, a post-combustion carbon capture process must be considered to capture both the CO_2 residual from the combustion process and the process chemistry.

The Danish government has recently constituted a commission to develop socio-economic sanctions with the purpose to reduce the national greenhouse gas emissions. These initiatives include a national CO_2 quota price as well as a sector-specific emissions tax. The variable emission taxes should accommodate specific sectors by reducing emission costs, such as mineralogical production processes as the cement production. The reduced taxes should prevent companies from relocating to other countries in order to achieve lower taxes (Svarer, 2022). The additional

costs associated with CO₂ emissions should promote the prevalence of CO₂ reducing solutions. Based on Aalborg Portland's current CO₂ emission, the increased costs will have major economic consequences, as shown in Table 1.1. Based on an expected annual CO₂ emission cost of 1.86 billion DKK, the incentive to lower the CO₂ emission by urgent actions is clear both from an environmental and an economic point of view.

Table 1.1: Estimated total emission cost for Aalborg Portland based on a quota price and the emission tax per ton of CO₂ for mineralogical processes, with data acquired from Aalborg Portland A/S (2019a) and UNESCO (2019)

Estimated CO₂ emission cost for Aalborg Portland	
CO ₂ quota price [DKK/ton]	750
Emission tax [DKK/ton]	100
Annually CO ₂ emission [ton/year]	2,189,152
Total emission cost [DKK/year]	1,860,799,200

From an international perspective, the International Energy Agency (IEA) has constructed a road map specifying possibilities to reduce the global CO₂ emission from cement plants (Benhelal et al., 2021). The road map enlightens CCUS as an initiative essential to lower the emission. CCUS aims to concentrate the CO₂ content from the off-gas before the high concentration CO₂ stream is utilised for either Power to X (PtX) or storage.

PtX is a process chain that utilises excess electricity to produce electrofuels with hydrogen extracted from electrolysis and captured CO₂ (Farfan et al., 2019). Consequently, by implementing an electrofuel synthesis facility with an associated electrolysis capacity, the CO₂ captured from the cement plant off-gas can be directly converted into useful fuels, which can be used internally at the cement plant. As a result, the captured CO₂ from the cement production is of high interest within the field of synthetic fuel production.

Thus, the necessity to reduce the CO₂ emission from the cement industry is evident, both from an environmental and economic point of view. Moreover, due to the high CO₂ emission from the process chemistry, a green fuel replacement

in the cement industry is not sufficient to remove the large CO₂ footprint. Thus, in order to capture the majority of the CO₂ emission from the cement industry, a post-combustion carbon capture technology must be implemented.

As a result, this report aims to find the most suitable post-combustion carbon capture technology to prevent CO₂ emission from the cement industry and simultaneously utilise the captured CO₂ in a PtX application for electrofuel production.

Chapter 2

Problem Analysis

In this chapter, the fundamentals of CCUS will be introduced along with different utilisation applications for the captured CO₂. Moreover, the incentive to investigate a point source, more specifically the cement plant off-gas will broadly be presented. Subsequently, different separation technologies with their respective advantages and disadvantage in combination with a PtX chain will be elaborated. The different treatment methods will be evaluated based on the existing literature, and the most suitable technology will be determined for further studies.

2.1 Introduction to CCUS

In Denmark, a 2030 objective has been adopted to reduce the CO₂ emission by 70 % compared to the emission level in 1990. In order to achieve this objective, significant changes must be implemented to existing and newly built CO₂ emitters. Consequently, the prevalence of carbon capture technologies is vital to achieving the 2030 objective (Energistyrelsen, 2020).

Captured CO₂ has been an integrated part of the oil industry since the 1970s, where it was used to enhanced oil recovery (Alvarado and Manrique, 2010). In recent years, research in carbon capture technologies has increased as a pathway towards achieving the climate goals (IEA, 2021), (Ku et al., 2020). In addition,

the prevalence of facilities for capturing CO₂ for either storage or utilisation has experienced an increase of 150 % over the last decades (IEA, 2021). The concept of CCUS combines the contribution of Carbon Capture and Storage (CCS) and Carbon Capture and Utilisation (CCU). The fundamentals of CCUS is illustrated in Figure 2.1.

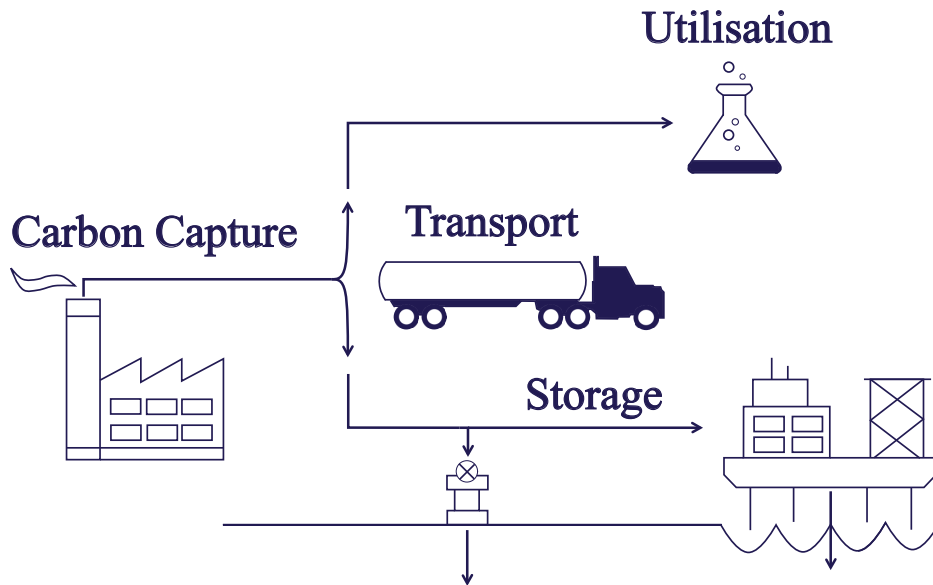
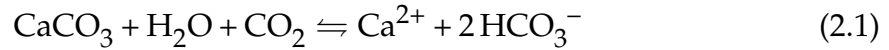


Figure 2.1: Conceptual illustration of the carbon capture, utilisation and storage.

As shown in Figure 2.1, the CO₂ is initially captured from a point source, such as a power or cement plant. The CO₂ capturing can be achieved with several technologies, which can be divided into mainly chemical and physical separation technologies (IEA, 2021), (Ku et al., 2020). Subsequently, the captured CO₂ is transported either to a storage or utilisation facility. The CO₂ can, for instance, be stored in emptied oil or gas reservoirs in the deep underground (IEA, 2021).

Another storage method is by dissolving the CO₂ in water and injecting the mixture into a basalt containing subsoil. Consequently, the CO₂ dissolved in water will react and form carbonic acid. By injecting the carbonic acid into a basalt containing subsoil, the basalt will dissolve and among other things form calcium oxide. The calcium oxide will react with CO₂ and form chalk, which appears in the bicarbonate formation presented in equation (2.1). According to the Icelandic CarbFix

project, the technology can store 95 % of the CO₂ injected into the subsoil within 2 years (IEA, 2021). This results in a very short monitoring period compared to the monitoring period for CO₂ stored in emptied oil reservoirs. The chemical reaction converting chalk extracted from basalt, water, and CO₂ into stable carbonate minerals which easily can be stored in the subsoil is shown in equation (2.1) (Matter et al., 2016).



Since approximately 10 % of the continental surface and ocean floor consists of basalt, this storage method is of high interest due to its accessibility (Matter et al., 2016). One of the disadvantages for this storing method is that freshwater is used instead of seawater, as freshwater can dissolve more CO₂ at the same pressure and temperature compared to seawater. According to Gislason et al. (2010), it requires 12 tons of seawater and only 10 tons of freshwater to dissolve 1 ton of CO₂. This poses an ethical issue as freshwater is considered an unsustainable supply (UNESCO, 2019). Thus, seawater must be used before it can be considered as a sustainable storing method. Combined with other CO₂ storage methods as well as different utilisation methods, the CO₂ reduction potential is evident and an important way to reach the CO₂ mitigation (Ghiat and Al-Ansari, 2021).

2.1.1 Carbon Capture and Utilisation

In support of CCS, CCU is considered an important CO₂ mitigation approach to achieve the CO₂ emission objectives. CCU has an advantage compared to CCS as CCU utilises a "waste product" to produce environmental friendly products, which promotes a great incentive to further investigation (Ghiat and Al-Ansari, 2021). The conversion of CO₂ into chemicals or electrofuels is an important utilisation pathway, representing a CO₂ sequestration potential of approximately 500 Mt/year (Chauvy et al., 2019). CCU represents various methods that utilise the captured CO₂ as a feedstock or for the generation of demanded commodities. There are several applications where the captured CO₂ can be utilised, for instance, to produce methane or methanol. Both methane and methanol can be produced through hydrogenation, where CO₂ and hydrogen are converted into useful fuels

which can participate in phasing out fossil fuels. The overall process chain from carbon capture to the electrofuel production is presented in Figure 2.2.

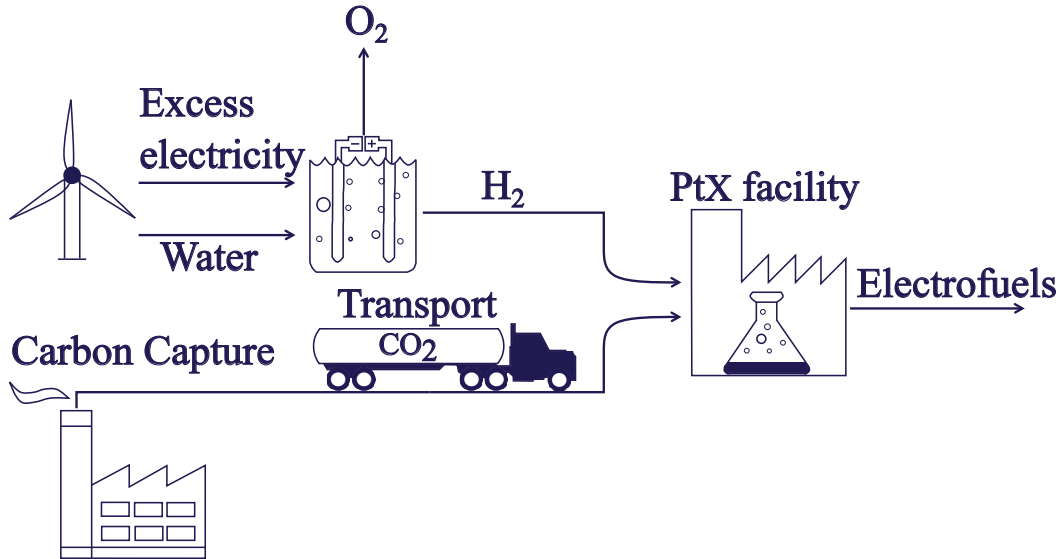
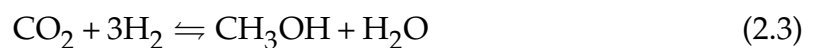


Figure 2.2: Conceptual illustration of the processes for electrofuel production.

It appears in Figure 2.2 that the Power to X (PtX) facility can utilise excess electricity to ionise water into hydrogen and oxygen through electrolysis, which forms the basis for electrofuel production. The chemical reactions transforming CO_2 and hydrogen into either methane or methanol are presented in equation (2.2) and (2.3), respectively.



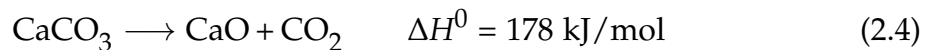
Since the reactants for both processes are the same, the end product depends solely on the catalyst. Consequently, carbon capture can preserve the environment but also contribute to the production of more sustainable energy sources. Ultimately, this increases the incentive to explore the possibility of capturing the CO_2 from the most appropriate point sources.

2.2 Cement Production Process

As stated in Chapter 1, the cement production accounts for 4 % of the Danish CO₂ emission and thus possesses a vital potential on the way to achieve the 2030 target of reducing the CO₂ emission by 70 %.

The cement production converts raw material, mainly consisting of limestone to clinker. The process occurs in several steps to obtain the high-quality clinker (Group, 2020). A simplified flow chart of the cement production is presented in Figure 2.3. The raw material utilised in the cement production consists of different minerals, primarily constituted of 83 % limestone, 5 % sand, and 4 % gypsum (Group, 2020). The first step of cement production is raw material processing, which accounts for several processes including; material crushing, storing, proportioning, and grinding. Subsequently, the raw mixture enters a preheater, which heat exchanges with an airflow from the clinker cooling. Afterwards, the mixture flows into a pre-calciner, which further heats the mixture before entering the rotary kiln. Due to the high temperature in the rotary kiln, a calcination reaction occurs. The temperature within both the pre-calciner and rotary kiln is established by a combustion process. The combustion characteristics are defined by the fuel used and the oxidiser, which typically is air.

The fuel is pre-treated prior to the combustion process in the fuel preparation process, where the fuel is dehumidified and ground to the desired fuel size (Bosoaga et al., 2009). Subsequently, the raw mixture is heated to 1,500 °C in the rotary kiln, which makes the limestone undergo the calcination reaction presented in equation (2.4).



The product of the rotary kiln is further cooled by heat-exchanging with the inlet airflow. Finally, the clinker undergoes the final processing to prepare the product for distribution and utilisation (Group, 2020), (Farfan et al., 2019), (Bosoaga et al., 2009). Figure 2.3 also indicates where the off-gas is discharged as well as the inlet oxidiser flow for the combustion process. The largest contributor to the

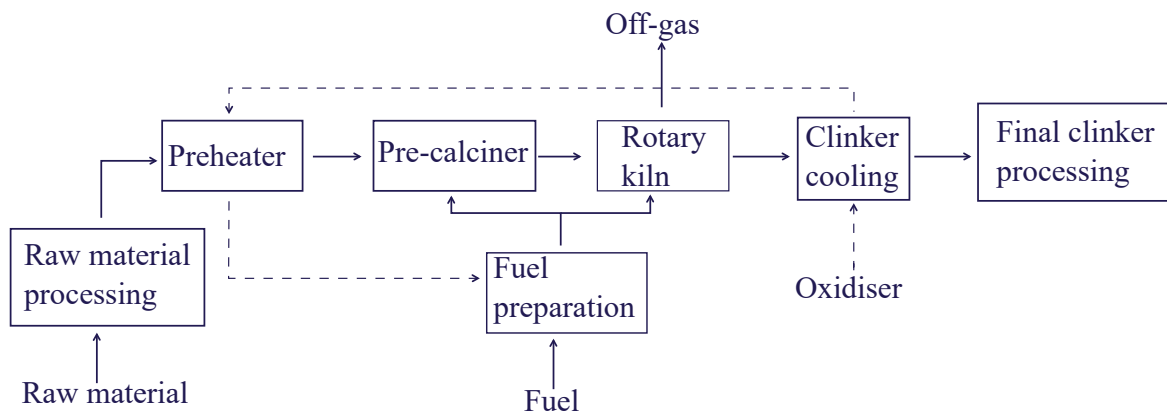


Figure 2.3: Flow chart of the cement production. The dotted line indicates the preheated oxidiser flow.

CO₂ emission is the calcination reactions which account for approximately 50 %. Subsequently, the combustion process accounts for approximately 40 % of the CO₂ emission. Finally, the use of electricity and transport constitutes the remaining 10 % of the CO₂ emission (Farfan et al., 2019), (Bosoaga et al., 2009).

The resulting cement plant off-gas composition discharged from the process is presented in Table 2.1 (Schakel et al., 2018), (Kær, 2019). The off-gas consists mostly of N₂, as it can be considered an inert gas in the combustion process. In addition, the second and third largest concentrations in the off-gas is H₂O and CO₂. Furthermore, the O₂ from the combustion is not fully reacted, as a small percentage remains in the off-gas. Finally, it appears from Table 2.1, that trace components of CO, NO_x, and SO₂ occur (Schakel et al., 2018).

Table 2.1: Estimated off-gas composition from a cement plant at 1,500 °C, with data acquired from Kær (2019) and Schakel et al. (2018).

Compound	Unit	Average value
CO ₂	mol.%	0.1739
O ₂	mol.%	0.0609
H ₂ O	mol.%	0.1304
N ₂	mol.%	0.6345
CO	ppm	1283
NO _x	ppm	133
SO ₂	ppm	19

However, it is assumed that the CO₂ emission from the calcination process is constant, due to the fixed amount of CO₂ bound in the limestone. As a result, the largest CO₂ contributor, which can be changed is the combustion process. Furthermore, several studies indicate that an increase in the CO₂ concentration in the off-gas is the most influential parameter affecting the capture energy duty (Mathisen et al., 2014). Consequently, an investigation of the combustion process in order to increase the CO₂ concentration is of high interest.

2.2.1 Introduction to Oxyfuel Combustion

As previously stated, the combustion process accounts for 40 % of the CO₂ emission from the cement production, which increases the incentive to investigate this process. Furthermore, it is assumed that the CO₂ emission from the calcination is constant and independent of the combustion process. Consequently, the focus is on improving the capture potential by adjusting the combustion process. The majority of the conventional combustion processes use air as the oxidiser, resulting in an oxygen supply of 21 %. However, by increasing the oxygen content in the oxidiser, an increased CO₂ concentration in the off-gas can be obtained, resulting in a higher potential for carbon capture. Due to the increased carbon capture potential, the possibility of increasing the oxygen concentration in the oxidiser will be considered (Hills et al., 2016). The oxygen supply could be covered from the

electrolysis process, in which the hydrogen for either methanol synthesis or methanation is produced. An increase in the oxygen concentration in the oxidiser will likewise result in a decrease in the fuel consumption. This is due to the fact that by increasing the oxygen concentration, the volume flow required to cover the combustion process with oxygen will likewise be reduced. The fuel consumption is reduced since less heat is used to heat up the inert nitrogen compounds (Dzurňák et al., 2021).

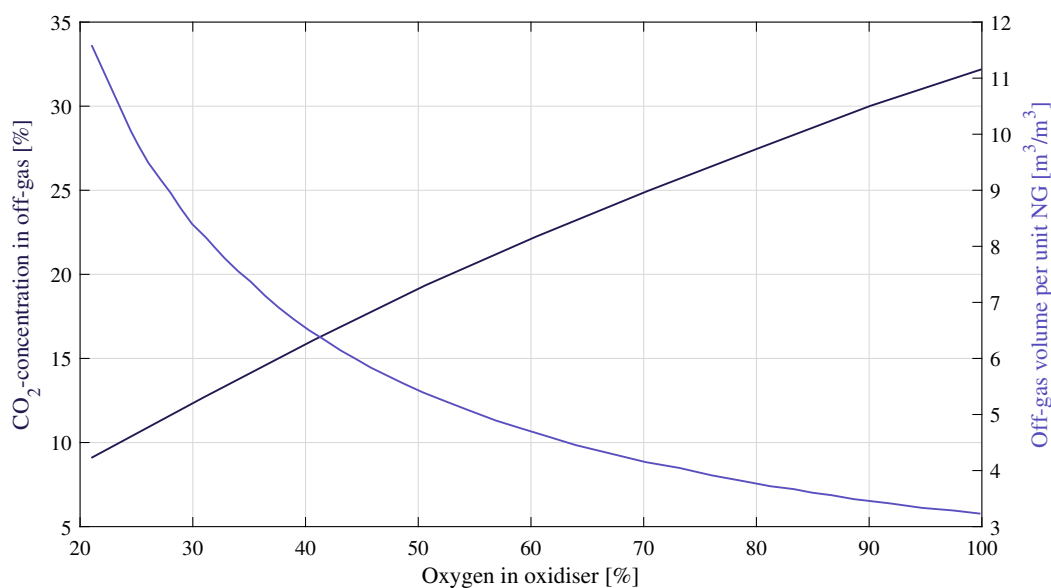


Figure 2.4: CO₂ concentration in the off-gas and off-gas volume per cubic meter natural gas (fuel) as a function of oxygen content in the oxidiser, based on data acquired from Dzurňák et al. (2019). The data is extracted from a combustion process fuelled by natural gas, but it is expected that the trends are equivalent for a coal fired combustion.

In addition, enhanced or complete oxyfuel combustion will likewise reduce the volume flow of the resulting off-gas up to 75 %, as shown in Figure 2.4. By reducing the volume flow, the scale of the treatment equipment will likewise be reduced, as it is scaled with regard to the volume flow (Wall, 2005). As a result, the total separation cost can be reduced by increasing the oxygen content in the oxidiser as it increases the CO₂ concentration in the off-gas and lowers the resulting volume flow. Based on these considerations, the combustion process will be further

investigated to determine a correlation between the oxygen content and the CO₂ concentration in the off-gas.

Additionally, independent of the combustion process, the cement industry must comply with the national emission limits. These criteria must prevent inappropriate emission of several harmful components into the environment. Conclusively, these emission limits must be complied with before oxyfuel combustion can be considered as an advantageous solution. The emission limits related to the components included in this report are presented in Table 2.2.

Table 2.2: Emission limits of harmful compounds for discharge to the environment (Aalborg Portland A/S, 2019b).

Legislation requirements	
Compound	Amount [Unit]
CO	1500 [ppm]
NO _x	500 [ppm]
SO _x	400 [ppm]

Consequently, the correlation between oxygen content in the oxidiser and the concentration of the vital compounds must be further investigated to avoid an inappropriate concentration of impurities and to maximise the CO₂ concentration in the off-gas. Additionally, in order to produce a usable CO₂ product, the captured CO₂ likewise needs to comply with some CO₂ purity requirements defined by the utilisation facility. Within the field of methane and methanol production, several compounds must be removed prior to the synthesis processes to ensure that the catalyst material does not deactivate.

2.3 CO₂ Purity Requirements for Electrofuel Production

To use the captured CO₂ for electrofuel production, several criteria must be met in order to obtain a usable CO₂ stream. These requirements are generally char-

acterised as the industrial CO₂ requirements. Concerning methanol or methane production, there is a special focus on the concentration of sulphur compound, due to the inhibitory effects on the catalyst material used to force the synthesis (Twigg and Spencer, 2003). In this report, the various carbon capture technologies are evaluated based on their ability to comply with the industrial CO₂ purity requirements. More specifically, the CO₂ must at least reach a purity of 99.5 mol.% and comply with the criteria for the minor components as presented in Table 2.3 (Brownsort, 2019).

Table 2.3: Purity requirements of the CO₂ stream for methane or methanol production Brownsort (2019).

Minor compounds	
Compound	Amount [Unit]
CO	2,000 [ppm]
O ₂	150 [ppm]
H ₂ O	50 [ppm]
NO _x	2.5 [ppm]
Sulphur	0.1 [ppm]

As stated in Table 2.3, the CO content has to be kept below 2,000 ppm to prevent corrosion and to reduce the consequences of a leak. Furthermore, the oxygen content must be kept below 150 ppm as it can catalyse corrosive components such as sulphur components (Brownsort, 2019). Moreover, the NO_x and sulphur content must be monitored and kept below the limits due to the fact that they can deteriorate the catalyst's ability to initiate the methanol or methane synthesis. By complying with the criteria presented in Table 2.3, no further treatment of the CO₂ stream is necessary before utilisation.

As a result, the off-gas composition and the requirements for utilisation will form the basis of the evaluation of the different separation technologies in order to find the most suitable technology.

2.4 Post-combustion CO₂ Capture Technologies

To obtain a sufficient CO₂ purity to supply the electrofuel synthesis, several separation technologies are considered. The fundamental of the separation process is to separate the CO₂ from the other impurities and concentrate the CO₂ stream for further utilisation. In this section, the following separation methods will be investigated; Amine scrubbing, Vacuum Pressure Swing Adsorption (VPSA), Cryogenic distillation, and Cryogenic solid-vapour separation. The technologies will be investigated to determine the most suitable separation process to produce liquefied CO₂ which is suitable for either storage on-site prior to utilisation or transportation to an external electrofuel facility. Furthermore, the separation technology must obey the industrial CO₂ purity requirement of 99.5 mol.%. Additionally, the technologies have to comply with the requirement regarding the minor component presented in Table 2.3. Eventually, the separation must obtain a CO₂ recovery of at least 99 %, to reach an acceptable separation rate and lower the emission from the cement plant. These assessment criteria will form the basis of the technology screening to find the most suitable technology, which will be selected for further investigation.

2.4.1 Amine Scrubbing

One of the most commercially used separation methods is the amine scrubbing technology, which uses an aqueous water/amine mixture to chemically bind the CO₂. Amines are ammonia derivatives, where one or more hydrogen molecules are released from the bindings. The released hydrogen molecules facilitate the chemical absorption of CO₂ (Dutcher et al., 2015). A schematic overview of the amine scrubbing process is illustrated in Figure 2.5.

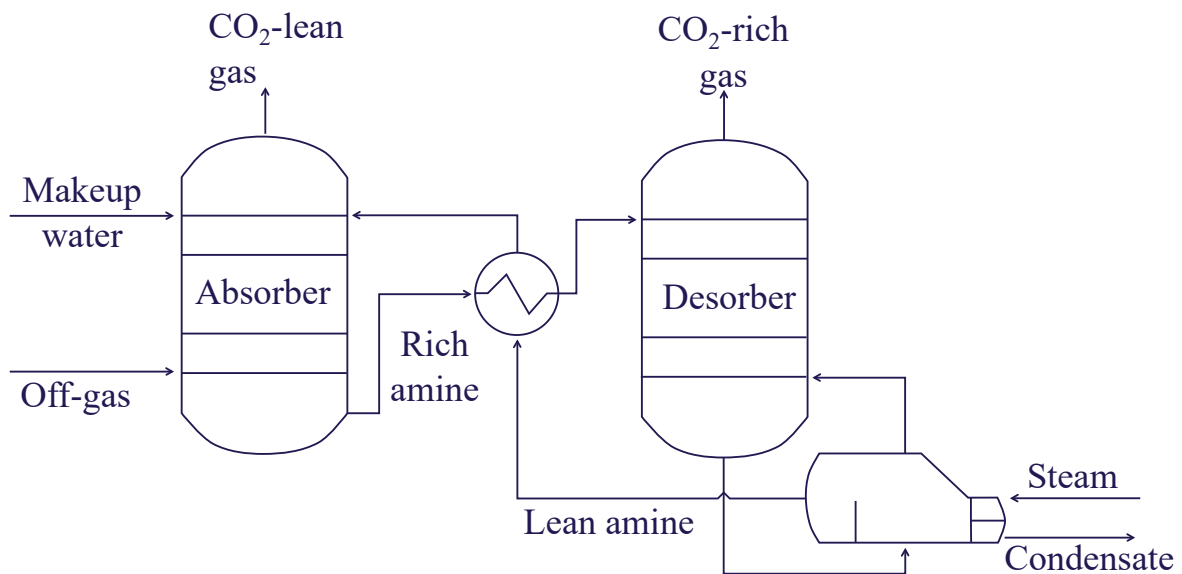


Figure 2.5: Schematic overview of the amine scrubbing technology, inspired by Dutcher et al. (2015).

The amine scrubbing technology is divided into two main parts, an absorber and a desorber, as presented in Figure 2.5. During the interaction between the off-gas and the amine mixture, the amines retain the CO₂ molecules from the off-gas. However, the majority of the remaining impurities will pass through the absorber and leave the system as a CO₂-lean off-gas. After the amines have bound a CO₂ molecule, they are referred to as rich amines. The rich amine mixture is further heated to approximately 120 °C to detach the CO₂ from the bindings. The specific temperature required to detach the CO₂ from the amines depends on the amine solvent used (Sartori, 1978). After the CO₂ is detached from the amines, the CO₂ stream can be released for further utilisation at a purity of 99.8 mol.% (Sutanto et al., 2017), (IECM, 2018). However, since the process releases the CO₂ in gaseous form, it will require a retrofitted liquefaction unit to convert the final product to liquefied CO₂ for either storage or transportation.

The amine regeneration process is the most energy-consuming part of the process. During the regeneration, the majority of the impurities which are bound to the amines are detached and can be removed as condensate. After the regeneration process, the lean amines are cooled and recycled into the absorber. The

amine solvent is cooled prior to the absorber to compensate for the heat generation produced by the exothermic reaction where amine binds CO₂ and in this way stabilises the temperature in the absorber (Dutcher et al., 2015). Due to the high heat consumption of the process, the use of surplus heat is crucial for the capture energy duty. Unfortunately, the majority of the excess heat can only be utilised for district heating in the winter period, which is a huge economic encumbrance in order to lower the capture energy duty. Thus, further possibilities for the use of surplus heat must be investigated, in order to make the amine process favourable. The resulting energy duty for the amine scrubbing technology is estimated to be 2.54 MJ/kg of captured CO₂ (Wang et al., 2013). Furthermore, according to a study conducted by Rao and Rubin (2002), SO₂ and NO_x will deteriorate the absorption ability of the amine solvent. As a result, pre-treatment of the off-gas is required to reach optimal separation conditions. Eventually, the amine scrubber technology can only reach a CO₂ recovery of 96 %, which is lower than the target recovery of 99 % presented in the assessment criteria. Conclusively, alternatives to amine scrubbing are of interest.

2.4.2 Vacuum Pressure Swing Adsorption

Vacuum Pressure Swing Adsorption (VPSA) is a commercially used gas separation technology, used in several applications, for instance for biogas upgrading and carbon capture. VPSA utilises elevated pressure to separate the CO₂ from the remaining compounds in the off-gas. A schematic overview of the separation process is presented in Figure 2.6. Initially, the off-gas is pressurised to obtain the desired separation pressure, which typically is between 8-12 bar (Speight, 2019). Subsequently, sulphur compounds are removed from the off-gas prior to the VPSA columns, as they will bind irreversibly to the adsorption material and degrade the separation ability. Due to the initial pressurisation, the water content can be removed as condensate.

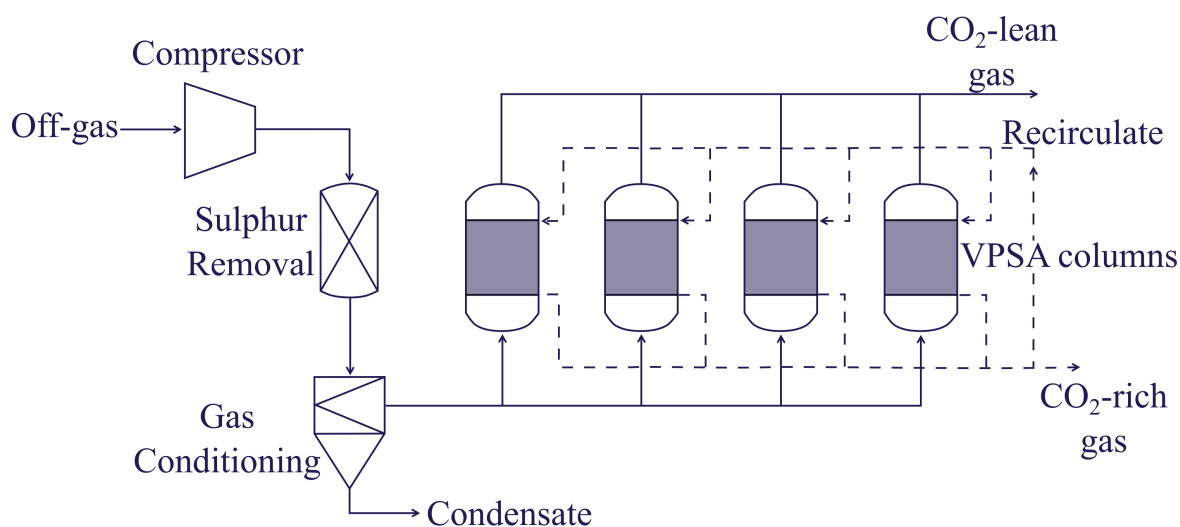


Figure 2.6: Schematic overview of the vacuum pressure swing adsorption technology.

The separation of the CO_2 occurs in the VPSA columns, where the CO_2 is extracted from the off-gas. The porous adsorption material retains the CO_2 , but not the remaining species from the off-gas. When the adsorption medium is saturated with CO_2 , the pressure is changed to vacuum conditions to release the CO_2 and regenerate the adsorption medium. To achieve a continuous process, several VPSA columns are required due to pressure-changing conditions during the regeneration process (Hoyer et al., 2016). The high concentration CO_2 stream is indicated with the dotted line in Figure 2.6. However, a fraction of the released CO_2 stream will be recirculated to achieve a higher CO_2 concentration. The VPSA separation method can purify the off-gas to a CO_2 concentration $> 95\%$ with a resulting energy duty of 2.44 MJ/kg of captured CO_2 (Wang et al., 2013). As a result, additional treatment is necessary to reach a CO_2 concentration that complies with the CO_2 purity requirements for methane or methanol production. However, by increasing the CO_2 concentration, the corresponding CO_2 recovery will decrease. Thus, a trade-off must be found between the desired CO_2 concentration and CO_2 recovery (Kozak et al., 2017). According to a study conducted by Kozak et al. (2017), the VPSA technology can only reach a CO_2 recovery of 76.4%, which is significantly below the 99% requirement. Furthermore, since the CO_2 is released as a gaseous phase at vacuum conditions, it will be an energy-consuming process to liquefy the CO_2 to achieve suitable conditions for further storage or transport.

Consequently, alternatives that are more suitable in order to obtain an sufficient CO₂ purity must be considered.

2.4.3 Cryogenic Distillation

Another conventional separation method is low-temperature separation, also known as cryogenic separation. Generally, the cryogenic separation technologies utilise low temperatures and differences in thermodynamic behaviour to separate the components. Cryogenic separation can obtain very high recovery of > 99 % with a CO₂ purity > 99.5 mol.% (Song et al., 2019). Within the field of cryogenic separation methods, several different technologies exist.

The most common technology is cryogenic distillation, which utilises the difference in boiling points to separate the components (Song et al., 2019). Commonly, the cryogenic distillation process appears as a cascade distillation to increase the purity and recovery. A schematic overview of a single stage cryogenic distillation process is presented in Figure 2.7.

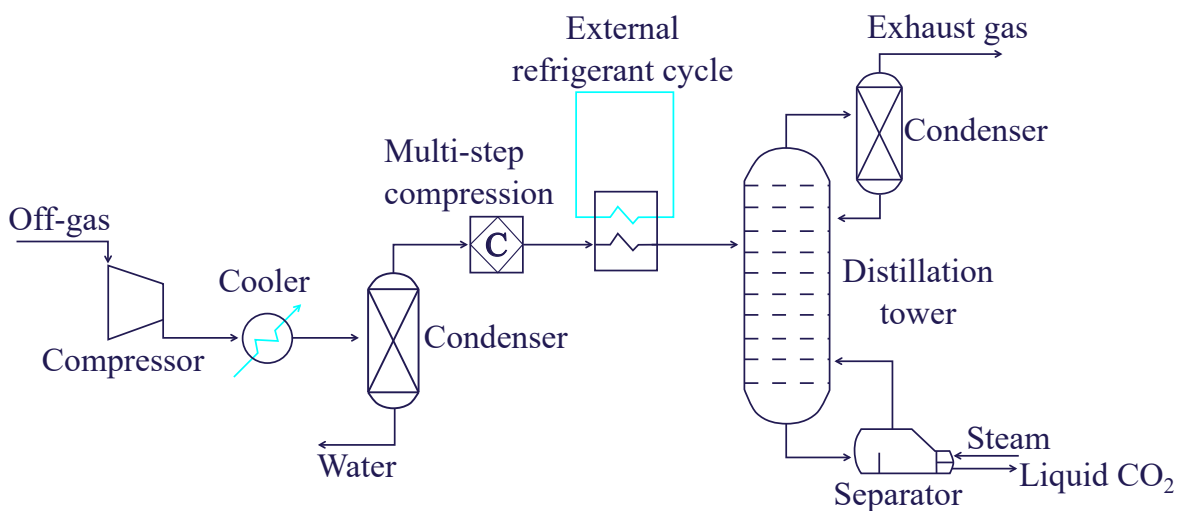


Figure 2.7: Schematic overview of a single stage cryogenic distillation process.

Initially, the off-gas passes through a compressor followed by a cooler to increase the pressure and lower the temperature. Afterwards, the off-gas is led through a condenser to separate the water from the off-gas, as water otherwise will freeze

and clog the system. Subsequently, the gas flows through a multi-step compression, in which the gas stepwise is compressed with internal cooling to above 45 bar (Pellegrini, 2014). Then, the flow is cooled below the boiling point for CO₂ at the desired pressure before the separation occurs in the distillation column. The separation occurs due to the difference in boiling points between CO₂ and the other impurities in the off-gas. The residuals from the distillation process are the CO₂-lean off-gas leaving the top as a gaseous phase and the liquid CO₂ in the bottom. The CO₂-lean off-gas is led through a condenser to recirculate the majority of the CO₂ which is not condensed. The liquid CO₂ phase enters a reboiler to ensure that the majority of the impurities dissolved in the liquid phase are recirculated to the distillation column. As a result, the purity of the liquid CO₂ stream increases before further utilisation (Song et al., 2019).

The disadvantage of the cryogenic distillation is the required pre-treatment for H₂O, SO_x, and NO_x prior to the distillation process. Furthermore, the multi-step compression is very energy-consuming as the off-gas is compressed at a gaseous state prior to the distillation column to reach the desired distillation conditions and to prevent dry-ice formation Aaron and Tsouris (2005). However, the advantage of cryogenic distillation is that the technology can obtain a recovery > 99 % with a corresponding CO₂ purity > 99.5 mol.%, and thus comply with the assessment criteria (Font-Palma et al., 2021). In addition, it is also an advantage that the CO₂ product is liquefied, as it increases the density and thus the suitability for either storage or transportation to an external utilisation facility. Furthermore, the resulting energy duty for the cryogenic distillation process is estimated to be 1.47 MJ/kg of captured CO₂, which is relatively low compared to the other conventional technologies (Font-Palma et al., 2021).

2.4.4 Cryogenic Solid-Vapour Separation

Alternatively to cryogenic distillation, cryogenic solid-vapour separation has shown promising initial results. According to Baxter et al. (2021), the cryogenic solid-vapour technology can lower the energy consumption for the carbon capture technology to 0.74 MJ/kg of captured CO₂, which is close to halving the energy con-

sumption compared to cryogenic distillation. However, this technology has not been used commercially yet, which indicates that further studies are needed to achieve a Technology Readiness Level (TRL) that allows it to be equated with commercial separation technologies.

The solid-vapour separation technology exploits that the compression of a solid is significantly less energy-consuming compared to a gas phase compression. As mentioned earlier, the multi-step compression required to prevent the dry-ice formation in cryogenic distillation accounts for a significant part of the energy consumption. This dry-ice formation is utilised to separate the CO₂ from the off-gas in cryogenic solid-vapour separation. Here, the off-gas is cooled to the CO₂ desublimation conditions, after which it can be separated due to solidification. Subsequently, the separated dry-ice is pressurised followed by a heat exchange, which carries out the melting process. The CO₂ phase diagram illustrates the desublimation, pressurisation, and melting process, presented in Figure 2.8.

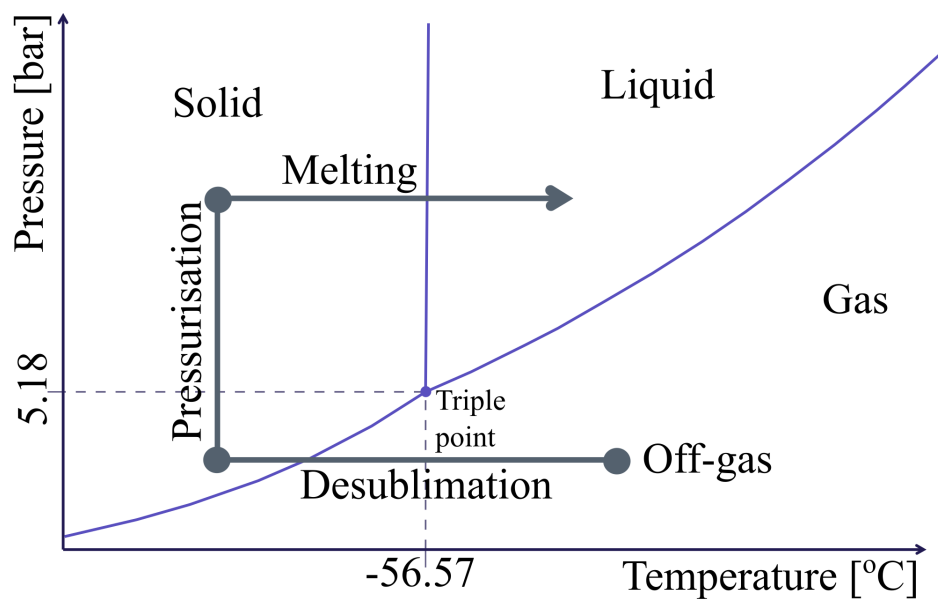


Figure 2.8: CO₂ phase diagram representing the phase behaviour during the cryogenic solid-vapour separation and subsequently liquefaction process.

A more detailed schematic overview of the cryogenic solid-vapour separation is

presented in Figure 2.9. Initially, the off-gas is dried to lower the water content. Subsequently, the off-gas enters a desublimation column at around $-100\text{ }^{\circ}\text{C}$ depending on both the CO_2 content and pressure. Inside the desublimation column, the CO_2 is captured from the off-gas due to the presence of cold contact liquid. The recovery of the CO_2 is very dependent on the temperature of the contact liquid (Baxter et al., 2021). The slurry leaving the desublimation column is pressurised to enhance the separation of the contact liquid and the solid CO_2 . Afterwards, the slurry enters a solid-liquid separator to extract the clean CO_2 product from the contact liquid. In addition, pure contact liquid can be recirculated to the desublimation column and close the separation process. The solid CO_2 is melted in the multi-stream heat exchanger before it enters a CO_2 polisher, which separates the remaining contact liquid to obtain a CO_2 concentration, which complies with the CO_2 purity requirements (Baxter et al., 2021).

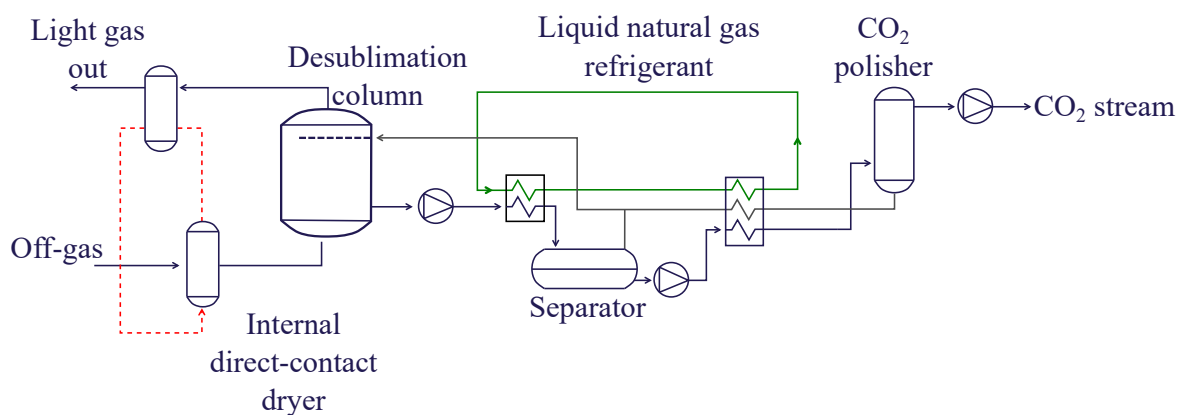


Figure 2.9: Schematic overview of the cryogenic solid-vapour separation with liquid natural gas as refrigerant, inspired by Baxter et al. (2021).

Since the CO_2 extracted from the process is liquefied, no additional energy supply is required to prepare the product for transport or storage, which is a huge advantage for the cryogenic solutions compared to both amine separation or VPSA. During the cryogenic solid-vapour separation, the off-gas is converted into a CO_2 -lean gas at ambient pressure and a liquid CO_2 stream at a pressure of 150 bar for further utilisation.

Another major advantage is the fact that the technology only consumes electricity, and no steam or other costly energy sources are required. According to Baxter et al. (2021), the technology can obtain a recovery > 99 % as well as a CO₂ purity of > 99.99 %, which means that no further treatment is necessary to comply with the CO₂ purity requirements. However, the main disadvantage of the technology is the low TRL. As a result, the technology requires further research and experimental studies to be considered a profitable and commercial technology that can be equated with other technologies (Baxter et al., 2021), (Font-Palma et al., 2021).

2.5 Evaluation of the Separation Methods

Amine scrubbing and VPSA are widely used technologies, but the cryogenic methods have some favourable advantages, which could be desirable for carbon capture solutions. Consequently, the most important advantages and disadvantages of the technologies with respect to the assessment criteria are presented in Table 2.4.

Table 2.4: Overview of the main advantages and disadvantages of the different carbon capture technologies.

Amine Scrubbing	
Pros	Cons
<ul style="list-style-type: none"> • The amine scrubber can reach a purity of 99.8 %. • Widely used with a high TRL. 	<ul style="list-style-type: none"> • Pre-treatment is necessary. • Requires utilisation of excess heat. • Liquefaction of the CO₂-stream is necessary for further use.
Vacuum Pressure Swing Adsorption	
Pros	Cons
<ul style="list-style-type: none"> • Requires only electrical energy. • Widely used with a high TRL. 	<ul style="list-style-type: none"> • The VPSA technology only reach a purity > 95 %. • Requires pre-treatment for sulphur compounds. • Can only reach a CO₂ recovery of 76.4 %.
Cryogenic Distillation	
Pros	Cons
<ul style="list-style-type: none"> • The CO₂ can reach a purity 99.9 %. • Liquefied CO₂ is suitable for further utilisation. • Require only electrical energy. 	<ul style="list-style-type: none"> • High investment cost. • Cryogenic conditions require high energy consumption. • High energy consumption.
Cryogenic Solid-Vapour Separation	
Pros	Cons
<ul style="list-style-type: none"> • Liquefied CO₂ is suitable for further utilisation. • Low energy consumption • Recovery and purity > 99.9 %. • Requires only electrical energy. 	<ul style="list-style-type: none"> • Not commercial utilised due to low TRL. • High investment cost

Table 2.4 shows that the VPSA technology will require further treatment to comply with the CO₂ purity requirements for electrofuel production. In addition, the

purified CO₂ flow will require a significant amount of pressurisation or cooling to achieve liquefied CO₂ for either storage or transportation. Alternatively, the amine technology can be used as it is the most widely used technology with the highest TRL. The disadvantage of the amine scrubbing technology is the excess heat from the regeneration process, which is difficult to utilise during the summer period. If the excess heat cannot be utilised, amine scrubbing is a very energy-consuming process. In addition, liquefaction of the purified CO₂ to obtain suitable conditions for storage or transportation will be very energy consuming, unless the electrofuel production occurs on-site.

Alternatively, the cryogenic solutions can achieve a high CO₂ purity of > 99.5 %, and thus comply with the desired CO₂ purity requirement. Furthermore, the outlet CO₂ product is liquefied, which is very favourable for storage or transportation before further utilisation. The disadvantages of the cryogenic solutions are the low TRL as well as high capital expenses (CAPEX). However, the cryogenic solid vapour separation technology has a significantly lower energy consumption compared to cryogenic distillation, as the concentrated CO₂ is pressurised after dry-ice formation, which reduces the energy consumption of the compression significantly. Conclusively, based on the established assessment criteria, cryogenic solid-vapour separation seems to be the most suitable technology. Consequently, this technology will be further investigated and form the basis of this report.

Chapter 3

Thesis Statement

Is cryogenic solid-vapour separation a suitable carbon capture technology for a cement plant off-gas in view of the technical potential, and is it possible to achieve synergistic effects between the cement production, the carbon capture technology, and the PtX integration?

3.1 Scope of the Project

To answer the thesis statement, the following will be covered:

- The composition of the off-gas from Aalborg Portland A/S is determined based on measurement data provided by Kær (2019).
- Models of the cryogenic solid-vapour separation technology, the calcination and combustion process, and the PtX integration will be developed.
- Energy optimisation for the cryogenic solid-vapour separation will be conducted with the associated constraints and heat integration.
- A sensitivity study of the modelled cryogenic solid-vapour separation and the combustion process will be conducted.
- An evaluation of the combined process train will be evaluated with respect to mass flow and corresponding energy consumption.

Chapter 4

Technical Analysis of the CCC Model

In this chapter, the estimated scale and off-gas composition from the cement production at Aalborg Portland is presented. The off-gas composition is inspired by Kær (2019) and will also include the most critical components with respect to electrofuel production presented in Table 2.3. These components are included to ensure that the final CO₂ product comply with the purity requirements for electrofuel production. The cryogenic solid-vapour separation process will in this report be referred to as the cryogenic carbon capture (CCC) process. The CCC process model will be presented and described in detail. The initial flow specifications used to approximate Aalborg Portland in terms of temperature, pressure, and mass flow rate are inspired by Kær (2019), Jensen (2015) and Aalborg Portland A/S (2019a). Subsequently, the immediate results extracted from the CCC model will be presented to give an overview of the flow specifications throughout the different stages. Eventually, the CCC model will be optimised in order to minimise the energy duty of the process. Finally, a sensitivity study of the CCC model will be conducted.

4.1 Scale and Composition

In this study, the off-gas composition and the corresponding flow specifications used to generate the initial results are an approximation of the grey cement production at Aalborg Portland inspired by (Kær, 2019). According to Kær (2019), the main components discharged from the calcination and combustion process are N_2 , O_2 , H_2O , and CO_2 . In addition, the presence of NO_x and SO_x are also included in the composition, as these components are considered critical both in terms of emission and to comply with the CO_2 purity requirement for utilisation. According to (L. Baxter, Personal communication, 1st April, 2022), it is expected that the amount of NO_x and SO_x is approximately 100 ppm each. Additionally, the initial off-gas temperature and pressure are estimated to be 70 °C and 1.07 bar (Jensen, 2015). This temperature is based on the fact that the hot off-gas discharged from the combustion and calcination process is used internally in the combustion process prior to the CCC process. Conclusively, the off-gas composition with the corresponding temperature and pressure is presented in Table 4.1.

Table 4.1: The chemical composition and flow specifications for the off-gas based on Jensen (2015), Kær (2019) and (L. Baxter, Personal communication, 1st April, 2022).

Off-gas composition	
Total flow [kg/h]	951,192
Temperature [°C]	70
Pressure [bar]	1.07
Mixture [mole fraction]	
Nitrogen	0.6345
CO_2	0.1739
Water	0.1304
Oxygen	0.0609
CO	0.001
Sulphur dioxide	0.0001
Nitrogen oxide	$5 \cdot 10^{-5}$
Nitrogen dioxide	$5 \cdot 10^{-5}$

4.2 Cryogenic Carbon Capture Model

The CCC process will be modelled using the steady-state process simulations software Aspen Plus[®]. By the use of Aspen Plus[®], it is possible to build a complex process model, which can take the thermodynamic behaviour into account. In Aspen Plus[®], the user specifies the equipment blocks, the thermodynamic models, and the inlet composition for the inlet streams. To approximate the thermodynamic behaviour, the user must specify an equation of state based on the compounds included, the temperature range, and the pressure range. Based on the selected equation of state, the flow properties, and the user specified equipment blocks, Aspen Plus[®] simulates the performance of the process (AspenTech, 2000).

To ensure that the process simulation approximates the actual phase behaviours during the simulation, an appropriate property method is necessary. When selecting the property method, the temperature, pressure, and compositions are crucial. Furthermore, to approximate the thermodynamic phase behaviour, the binary interaction coefficients for all the compounds must be available in the property method. The compounds represented in the off-gas are listed in Table 4.1. Based on the compounds represented in the off-gas and the cryogenic operating temperatures, the Peng-Robinson (PENG-ROB) property method is selected. The PENG-ROB is validated during cryogenic conditions and includes all the binary interaction coefficients between the compounds presented in Table 4.1 (Jensen, 2015).

The PENG-ROB property method uses the Peng-Robinson cubic equation of state to calculate the thermodynamic properties (AspenTech, 2001). Additionally, the included binary interaction coefficients increase the accuracy of the phase equilibria. Generally, the PENG-ROB property method is best suitable for nonpolar or mildly polar mixtures, for instance, hydrocarbon, CO₂, and hydrogen. Furthermore, the property method can generate reasonable results within all temperatures and pressures, however with the least accuracy near the critical point (AspenTech, 2001). Based on all the considerations, the PENG-ROB property method is selected and utilised to approximate the phase equilibria during the CCC process.

4.2.1 CCC System Description

Based on the composition described in Table 4.1, the selected property method, and the CO₂ purity requirements, the CCC model can be developed in Aspen Plus[®] as shown in Figure 4.1. The model consists of several components whose common purpose is to separate the CO₂ from the cement plant off-gas. The entire process model is attached as Supplementary 1. In addition, to simplify the process modelling as well as ensure that the process operates under reasonable conditions, the following assumptions have been made:

- The pressure ratio in the compressors cannot exceed 3 suggested by (Dincer and Zamfirescu, 2014).
- The minimum pinch temperature in the heat exchangers is 2 °C following cryogenic conditions.
- The pressure loss in the heat exchangers or coolers is neglected.
- The compressors are estimated to have an efficiency of 72 %, which is the default in Aspen Plus[®].
- The majority of the minor components are not included in the off-gas composition unless they are considered critical for the electrofuel production.

These assumptions will provide the basis of the CCC process modelling presented in Figure 4.1. Furthermore, the CCC model is divided into three sub-components, which represent the desublimation column, the melter, as well as the final treatment process.

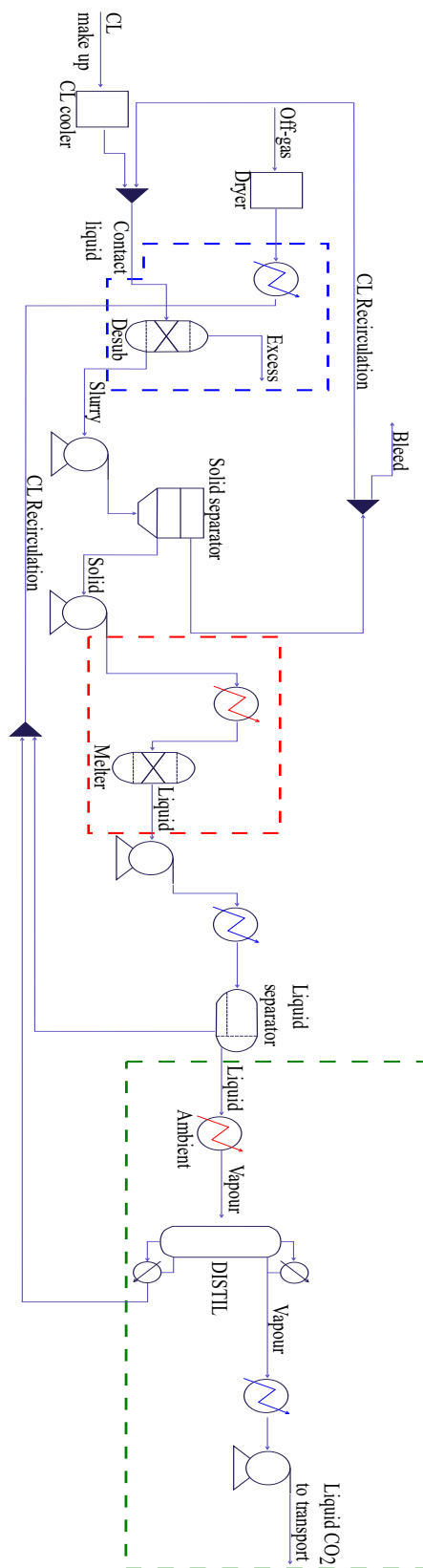


Figure 4.1: Schematic overview of the cryogenic carbon capture model developed in Aspen Plus®. The blue dotted line encapsulates the desublimation process of the model, whereas the red dotted line frames the melting process. Finally, the green dotted line encapsulates the last treatment step before pressurisation to transport. Additionally, the dryer component and the contact liquid refrigerant circuit are further elaborated in Appendix A.

Initially, the cement plant off-gas enters the system at 70 °C and 1.07 bar inspired by Kær (2019) and Jensen (2015). The relatively low inlet temperature has been used, as it is expected that the majority of the excess heat from the off-gas has been used internally in the cement production. The first part of the system is a dryer component, which consists of several flash stages. The dryer component removes the water content to prevent clogging of the system when low temperatures are desired. An elaborated description of the dryer component is presented in Appendix A. After the flash stages in the dryer component, the water content in the off-gas is removed. However, several impurities are dissolved in the removed water. As a result, the water discharged from the system needs further treatment before it can be discharged to the environment. However, the water treatment to comply with the emission limits is not investigated in this report.

After the dryer component, the dehydrated off-gas enters a heat exchanger at 10 °C and is further cooled to -100 °C. A focused schematic overview of the desublimation equipment with the associated temperature profile is presented in Figure 4.2a and 4.2b. The temperature profile illustrates the decrease in temperature due to the heat exchanger as the initial decrease. The desublimation of CO₂ occurs, followed by interaction with the cold contact liquid. The contact liquid is cooled to -125 °C in an external refrigerant circuit prior to the injection into the desublimation column. The external refrigerant circuit is elaborated in Appendix A. Moreover, the desublimation phase change is illustrated as the more flattened part of the temperature profile. However, due to the presence of impurities in the gas, the temperature will slightly decrease during the desublimation of CO₂.

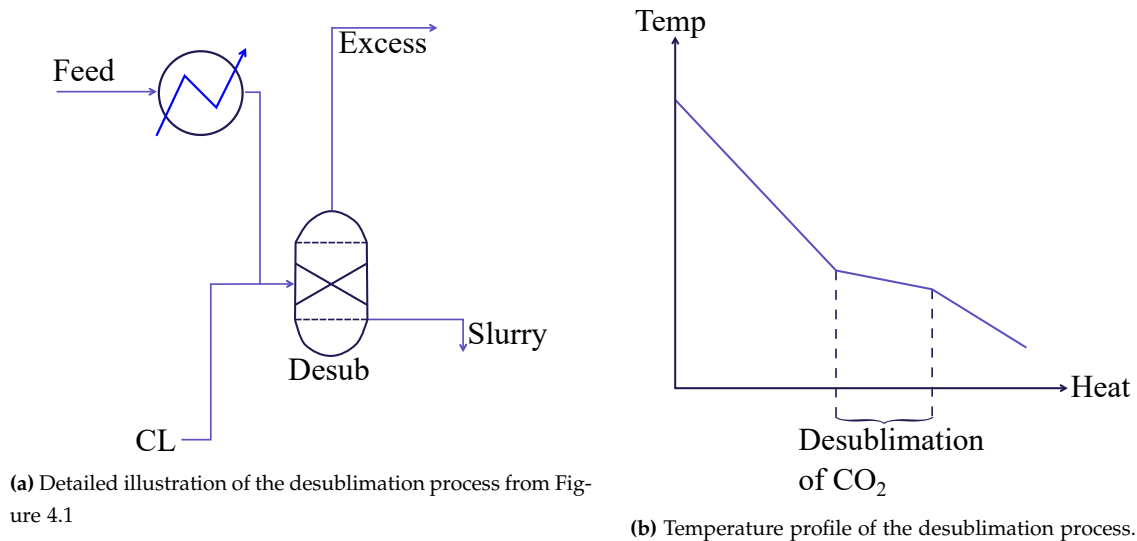


Figure 4.2: Schematic overview of the desublimation process with the resulting temperature profile throughout the desublimation process.

Inspired by a report conducted by Jensen (2015), the desublimation column in the Aspen Plus[®] model is represented by a Gibbs reactor. However, a conceptual drawing of a desublimation column is shown in Figure 4.3. The desublimation column works as a combined heat exchanger and a CO₂ separator.

Initially, the off-gas is injected from the bottom of the desublimation column before it moves towards the top due to buoyancy. Simultaneously, the contact liquid is sprayed over the gas from the top. Due to the temperature and pressure inside the column, the CO₂ will desublimates from a gaseous phase to a solid during the interaction with the contact liquid. When the CO₂ desublimates, it will precipitate as a slurry in the contact liquid and leave the system from the bottom of the column, as shown in Figure 4.3.

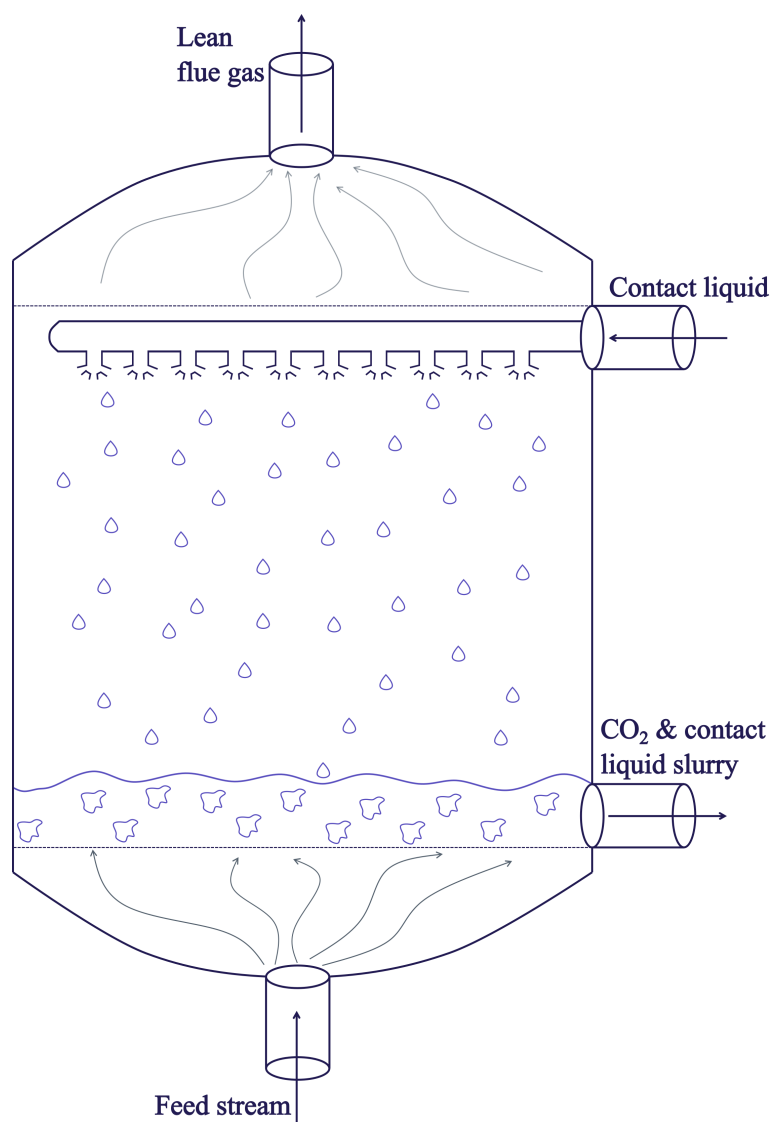
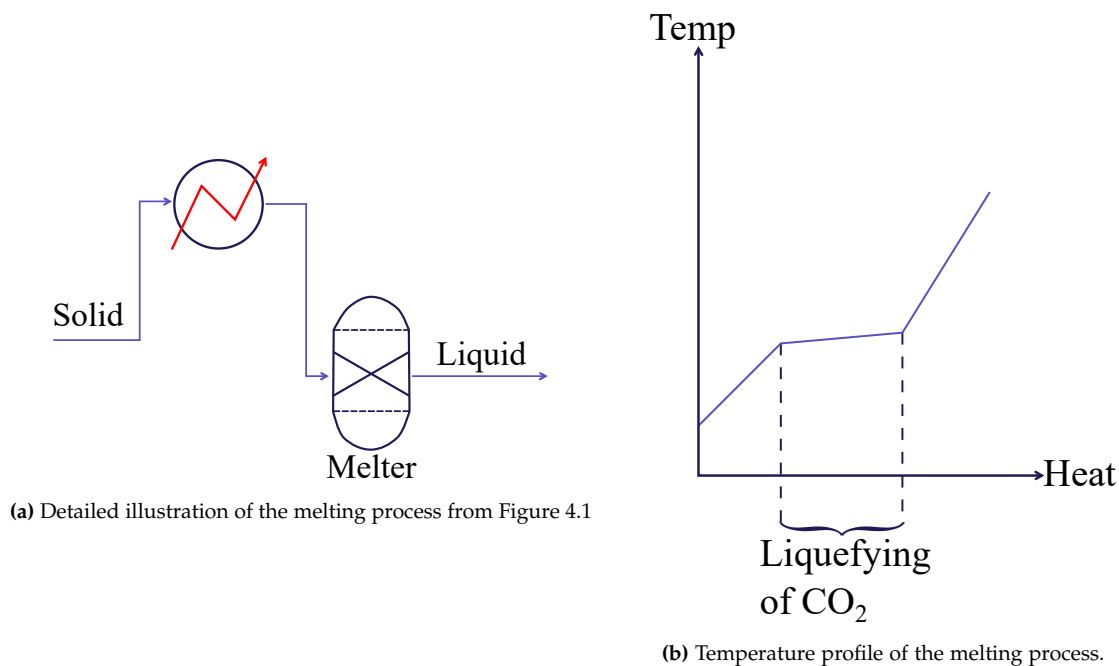


Figure 4.3: Conceptual illustration of the desublimation column.

After the CO₂ separation in the desublimation column, an exhaust gas consisting of the remaining compounds is discharged. The slurry of contact liquid and CO₂ is further pressurised to improve the separation in the solid separator. Subsequently, the separated contact liquid is recirculated in order to reduce the make-up flow needed to sustain the CO₂ separation. However, a fraction of the impurities and the CO₂ will remain in the contact liquid stream. Thus, a bleed is needed to prevent an accumulation of impurities in the system. To compensate for the bleed,

the recirculated contact liquid is mixed with a make-up flow of pure contact liquid.

After the solid separator, a mixture of mostly solid CO_2 and contact liquid is discharged for further treatment at a temperature of $-119\text{ }^\circ\text{C}$ and a pressure of 7 bar. The mixture is further compressed in a screw-pump to prevent clogging, before it enters the melting process marked with the red dotted line in Figure 4.1. A focused illustration of the melting process is presented in Figure 4.4a. Additionally, the associated temperature profile for the melting process is illustrated in Figure 4.4b.



(a) Detailed illustration of the melting process from Figure 4.1

(b) Temperature profile of the melting process.

Figure 4.4: Schematic overview of the melting process and the resulting temperature profile.

The melting process is illustrated with a heat exchanger and a Gibbs reactor to force the phase change. The solid-liquid mixture enters the heat exchanger at $-119\text{ }^\circ\text{C}$ and is heated to $-50\text{ }^\circ\text{C}$ to achieve a liquid state. However, to obtain the phase change from solid to liquid, a Gibbs reactor is necessary due to the fact that the heat exchangers in Aspen Plus[®] cannot manage solid-liquid phase change.

Subsequently, the liquid CO_2 is pressurised to 30 bar and cooled before it enters a decanter, which is a liquid-liquid separator that separates the two immiscible

liquids based on densities. The pressurisation prior to the decanter occurs due to the fact that it will increase the degree of separation. Within the decanter, the liquid CO₂ is purified to approximately 99.2 mol.%, whereas the remaining impurities primarily consist of contact liquid. As a result, the purified CO₂ stream needs further treatment to comply with the CO₂ purity requirements. Consequently, the liquid CO₂ stream is further heated to around 5 °C to make a phase change into a gaseous phase by heat exchanging with ambient air. Subsequently, the final treatment of the CO₂ stream occurs in a distillation column, as shown in Figure 4.5.

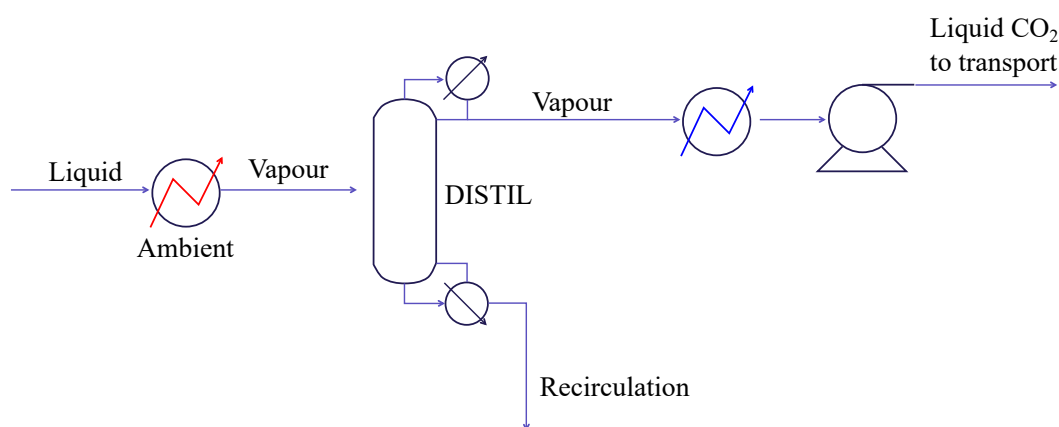


Figure 4.5: Focused illustration of the final separation and pressurising of the CO₂ before it is sent to transport indicated by the green dotted line in Figure 4.1.

The distillation column separates the CO₂ from the impurities based on the difference in boiling points. The number of trays and the optimal inlet stage is determined to be 28 and 14, respectively, based on a sensitivity study accomplished in Aspen Plus[®]. Furthermore, the distillation temperature and pressure must be specified to ensure that the components are separated at the desired conditions. Moreover, a reboiler is included in the bottom of the distillation column to recycle the majority of the CO₂ dissolved in the liquid leaving the column. Additionally, a condenser is likewise included to recycle the majority of the impurities leaving the distillation column with the gaseous CO₂ stream to increase the final CO₂ purity. To achieve the desired separation conditions, the reboiler pressure is set to 28.5 bar, whereas the condenser pressure is specified at 30.1 bar. After the distillation column, the CO₂ stream has reached a concentration of 99.96 mol.%, which

is sufficient for further utilisation. After the distillation process, the purified CO₂ stream is cooled to approximately -5 °C to obtain a liquid phase stream before the final pressurisation. The liquid CO₂ stream is pressurised to 150 bar to comply with the common liquefied CO₂ transportation conditions.

In Table 4.2, the initial results based on the cement plant off-gas composition from Table 4.1 are presented. Specifically, the total flow, CO₂ flow, and gas composition through the most important components are presented.

Table 4.2: Comparison between the flow specifications for the cement plant off-gas and CO₂ outlet stream with the corresponding composition throughout the different stages in the CCC model.

Flow comparison between the cement plant off-gas and the CO₂ outlet stream						
	Off-gas stream			CO₂ outlet stream		
Total flow [kg/h]	951,191			244,861		
CO ₂ flow [kg/h]	244,798			244,796		
Results of the composition through the CCC model						
Compounds [mol.%]	OFF-GAS	DRYER	DESUB	SOLID	LIQSEP	DISTL
Nitrogen	62.5	71.8	0.296	0.0244	0.0231	0.0251
Water	13.05	0	0	0	0	0
CO ₂	17.4	20.0	4.10	92.1	98.3	99.96
Oxygen	6.09	7.00	0.168	0.0139	0.0129	0.0140
Sulphur dioxide	0.01	0.0115	0.208	0.0171	0.0177	0
Nitrogen oxide	5·10 ⁻³	5.75·10 ⁻³	1.15·10 ⁻²⁹	2.59·10 ⁻²⁸	0	0
Nitrogen dioxide	5·10 ⁻³	5.55·10 ⁻³	9.32·10 ⁻¹⁰	7.67·10 ⁻¹¹	2.66·10 ⁻¹⁰	0
Contact liquid	0	0	95.2	7.83	1.67	0
CO	1.0	1.1	0.0108	8.89·10 ⁻⁴	7.86·10 ⁻⁴	8.53·10 ⁻⁴
HCL	1·10 ⁻⁵	0	0	0	0	0

Based on the intermediate results presented in Table 4.2, it appears that the CCC model can achieve a recovery of 99.9 % with a corresponding CO₂ purity of 99.6 mol.%. Furthermore, to minimise the resulting energy duty and still comply with the CO₂ purity requirements, an energy optimisation will be conducted.

4.3 Optimisation of the CCC Model

The CCC model is energy optimised to lower the energy consumption for the capture technology. Firstly, the optimisation procedure is presented with the associated case-specific considerations. Afterwards, an objective function is generated, accounting for the total energy consumption of the CCC model. Subsequently, the adjustable parameters influencing the objective function are stated with their corresponding boundary conditions. The boundary conditions are inspired by empirical literature and are specified to prevent inappropriate phase shifts and ensure a reasonable optimum is found. Additionally, the results of the energy optimisation are presented and evaluated. Finally, heat integration of the CCC model will be investigated, and the energy duty per kg of captured CO₂ is compared to empirical values for conventional capture technologies.

The energy optimisation is preferred instead of a cost optimisation since vital equipment in the CCC process is replaced with Gibbs reactors to approximate the desublimation column and the melter component. Considering these simplifications, it is expected that the cost evaluation with Aspen Process Economic Analyser (APEA) will be uncertain both in terms of CAPEX and OPEX. Furthermore, by minimising the energy consumption within the system, it is expected that the corresponding Equivalent Annual Cost (EAC) will go towards a minimum, due to the strong correlation presented in Baxter et al. (2021). Based on these considerations, the optimisation can be conducted in the following steps:

1. Identify adjustable parameters which affect the energy consumption of the CCC model.
2. Generate an objective function based on the identified adjustable parameters.
3. Identify constraints of the model.
4. Optimise the problem using the optimising tool in Aspen Plus[®].
5. Evaluate the optimised results concerning the energy consumption.

The purpose of the optimisation process is to obtain the lowest possible energy consumption of the system and still comply with the CO₂ purity requirements stated in Table 2.3. The first step is to identify the adjustable parameters influencing the energy consumption. These parameters with their associated optimisation range are presented in Table 4.3.

Table 4.3: The adjustable parameters and their associated bounded ranges from the CCC model.

Adjustable parameters		
Parameter	Initial value	Ranges
Reboiler pressure [bar]	28.5	26.5 - 30.5
Condenser pressure [bar]	30.1	28.1 - 32.1
Reflux ratio [-]	4.17	2 - 5
Desublimation temperature [°C]	-120	(-135) - (-120)
Desublimation pressure [bar]	1.07	1.01 - 3
Solid separator pressure [bar]	9	7 - 10
HEX temperature [°C]	-100	(-110) - (-90)
HEX-1 temperature [°C]	-50	(-60) - (-40)
HEX-2 temperature [°C]	-87.65	(-90) - (-80)
HEX-3 temperature [°C]	5	3 - 7
HEX-4 temperature [°C]	-10	(-12) - (-8)
Dryer HEX temperature [°C]	10	8 - 12
Dryer HEX-1 temperature [°C]	10	8 - 12
Dryer HEX-2 temperature [°C]	5	3 - 7

Subsequently, an objective function can be generated by summarising the energy consumption of all the equipment block represented in the CCC model. Furthermore, the objective function is based on absolute values, since cooling appears as a negative energy duty, which must be considered as an energy expense for the system. As a result, the total energy consumption of the CCC technology can be

minimised by minimising the objective function presented in equation (4.1).

$$Obj = |\dot{Q}_{reboil}| + |\dot{Q}_{cond}| + |\dot{Q}_{Desub}| + |\dot{Q}_{Melt}| + |\dot{Q}_{HEX}| + |\dot{Q}_{HEX-1}| + \dots \\ |\dot{Q}_{HEX-2}| + |\dot{Q}_{HEX-3}| + |\dot{Q}_{HEX-4}| + |\dot{Q}_{Dry,HEX}| + |\dot{Q}_{Dry,HEX-1}| + |\dot{Q}_{Dry,HEX-2}| \quad (4.1)$$

Based on the objective function, the minimum energy consumption can be found by adjusting the adjustable parameters within the bounded ranges. However, to ensure that the captured CO₂ comply with the purity requirements, several constraints must be specified. The constraints are based on the CO₂ purity requirements presented in Table 2.3, and listed from equation (4.2) to equation (4.8).

$$c_1 = y_{CO_2} - 0.995 \quad (4.2)$$

$$c_2 = 1 \cdot 10^{-9} - y_{HCL} \quad (4.3)$$

$$c_3 = 0.002 - y_{CO} \quad (4.4)$$

$$c_4 = 4.021 \cdot 10^{-8} - (y_{NO} + y_{NO_2}) \quad (4.5)$$

$$c_5 = 1 \cdot 10^{-7} - y_{SO_2} \quad (4.6)$$

$$c_6 = 0.00015 - y_{O_2} \quad (4.7)$$

$$c_7 = 0.05 - y_{H_2O} \quad (4.8)$$

The constraints from c_1 to c_6 ensures that separated CO₂ stream meets the purity requirements. In addition, c_7 restricts the water content prior to the water knock-out in the dryer component presented in Appendix A. This constraint should ensure that the off-gas can be considered sufficiently dehydrated before entering the CCC process to prevent ice formation.

Based on the identified adjustable parameters and the specified constraints, the BOBYQA optimisation algorithm can be executed to minimise the objective function. The BOBYQA optimisation algorithm is used in Aspen Plus[®] due to its high robustness. The resulting values from the optimisation performed in Aspen Plus[®] are presented in Table 4.4.

Table 4.4: The resulting optimised values for the adjustable parameters and the constraints.

Adjustable parameters	
Parameter	Optimised value
Reboiler pressure [bar]	26.5
Condenser pressure [bar]	32.1
Reflux ratio [-]	2
Desublimation temperature [°C]	-120
Solid separator pressure [bar]	7
HEX temperature [°C]	-97.31
HEX-1 temperature [°C]	-49.88
HEX-2 temperature [°C]	-80
HEX-3 temperature [°C]	7
HEX-4 temperature [°C]	-8
Dryer HEX temperature [°C]	12
Dryer HEX-1 temperature [°C]	12
Dryer HEX-2 temperature [°C]	4.71
Constraints	
Parameter	Optimised value
CO ₂ mole fraction	0.9995
HCL mole fraction	0
CO mole fraction	$8.98 \cdot 10^{-6}$
NO _x mole fraction	0
SO ₂ mole fraction	0
O ₂ mole fraction	0.00015
Water mole fraction	0.0031

Based on the minimisation of the objective function, the associated optimised parameters and constraints can be found. By minimising the numerical value of the objective, the lowest possible energy consumption for the CCC model can be determined. Thus, the resulting minimised objective function value is determined to be 429 MW. Consequently, based on the total energy consumption of the CCC process, the associated energy duty per kg captured CO₂ can be determined to

5.77 MJ/kg of captured CO₂. The resulting optimised CO₂ outlet stream and the corresponding CO₂ recovery are presented in Table 4.5.

Table 4.5: Optimised results regarding the CO₂ recovery and the CO₂ outlet stream composition.

Optimised results of CO₂ outlet stream	
Recovery [%]	99.9
Compounds [mol.%]	
Nitrogen	0.0251
CO ₂	99.96
Oxygen	0.0140
CO	$8.53 \cdot 10^{-4}$
Sulphur oxide	-
Nitrogen oxide	-
Nitrogen dioxide	-

However, the energy optimisation does not take internal heat integration into account, which can have a major impact on the total energy consumption. Consequently, to identify the potential for heat integration in the CCC process, a pinch analysis will be conducted.

4.4 Heat Integration

The potential for heat integration is investigated in order to identify the ideal heat recovery. The pinch analysis is performed based on a pinch temperature of 2 °C, since the pinch point is found under cryogenic conditions (L. Baxter, Personal Communication, 1st April, 2022). The pinch analysis is performed based on the heat consumption and the corresponding temperature intervals from the CCC process modelled in Aspen Plus[®]. The resulting composite curves from the pinch analysis is presented in Figure 4.6 and is further elaborated in Supplementary 2. The red composite curve in Figure 4.6 represents the hot streams which require cooling whereas the blue curve represents the cold streams which require heating.

Moreover, the surplus heat appears below the pinch point and represents the heat which is not utilised within the system.

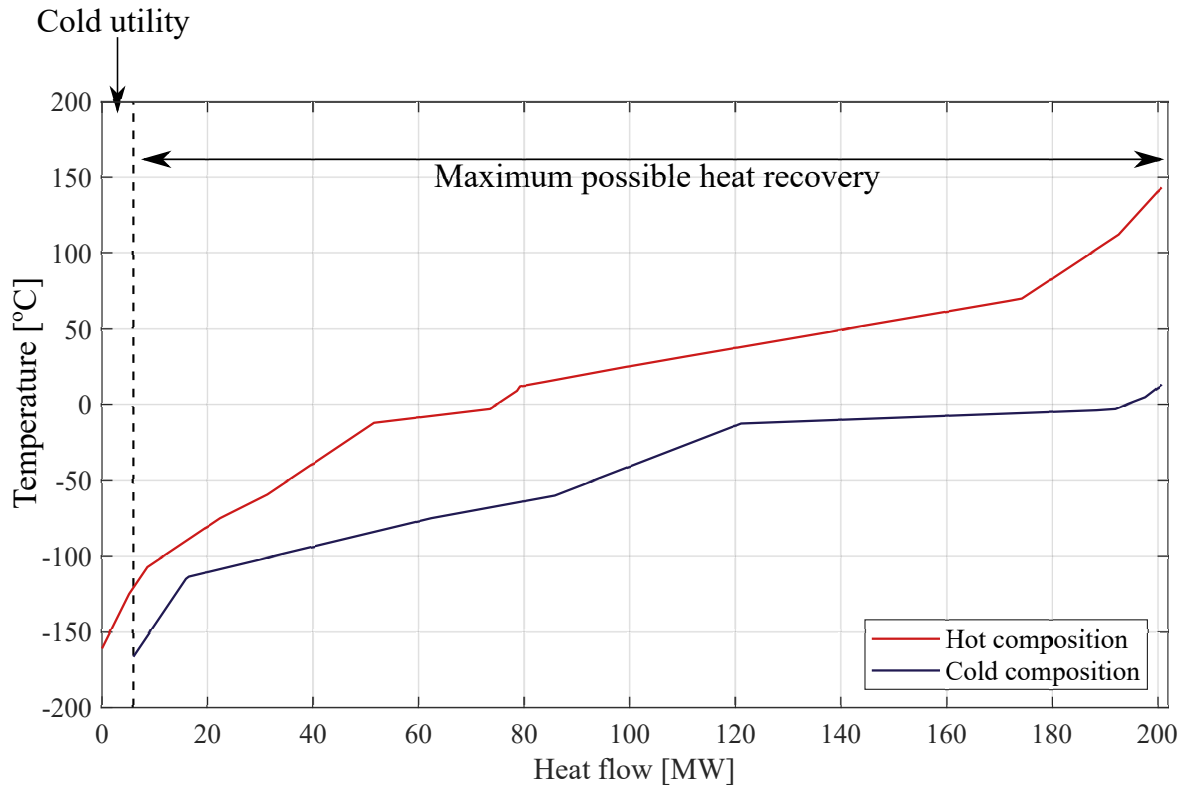


Figure 4.6: Composite curves illustrating the maximum possible heat recovery for the CCC model. The cold utility amounts to 5.95 MW.

The overlapping part of the composite curves indicates the maximum possible heat recovery within the system. Based on the heat integration analysis, it appears that the entire cold composite curve can be covered by heat exchanging with the hot streams within the system. Thus, if the ideal heat recovery is taken into account, the total energy consumption can be reduced with 84.6 %, resulting in a energy duty of 0.89 MJ/kg-captured CO₂. Consequently, based on the results from the pinch analysis, it appears that heat integration must be taken into account when designing the CCC process.

A schematic overview of the energy duties from different carbon capture technologies are presented in Figure 4.7. The energy duty of the empirical CCC model

is based on Font-Palma et al. (2021) whereas the other conventional technologies are based on Wang et al. (2013). By comparing the energy duties from the technologies presented in Chapter 2, it appears that the CCC technology is the most competitive solution. In addition, the theoretical minimum energy duty for CO₂ separation is likewise presented in Figure 4.7, represented by the dotted line. The theoretical minimum energy duty is evaluated based on the energy required to force the CO₂ phase changes and the energy required to compress the separated CO₂ stream to 150 bar, which is equivalent to the outlet pressure achieved in the modelled CCC process (Berger et al., 2020). According to Berger et al. (2020), the theoretical minimum energy duty for CO₂ separation is 0.375 MJ/kg-CO₂, which can be considered as the theoretical zero point.

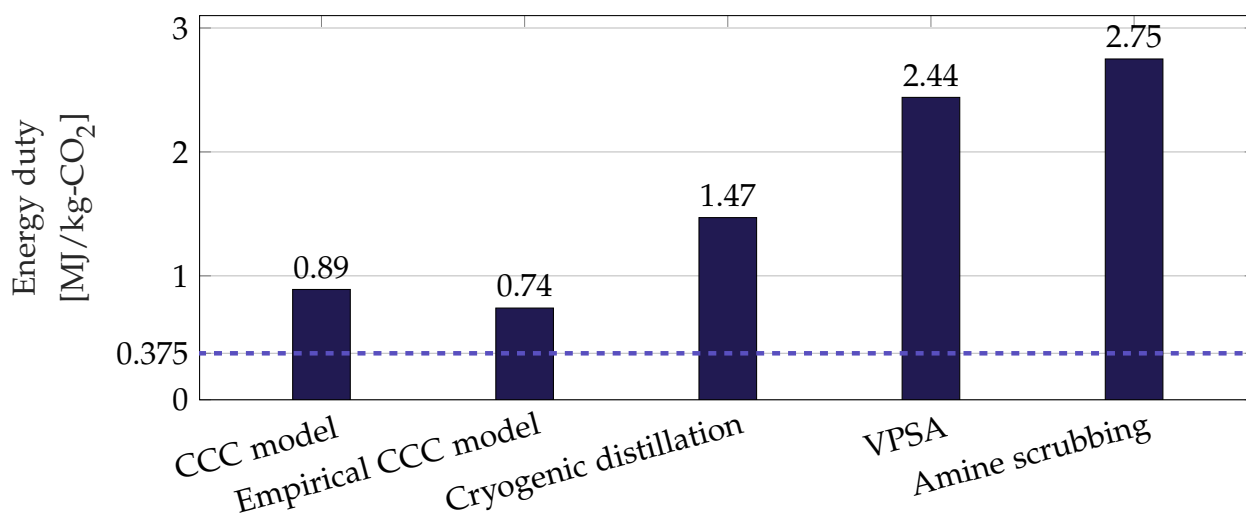


Figure 4.7: Comparison of the energy duties between the developed CCC model and the carbon capture technologies described in Chapter 2. The energy duties of the technologies other than the CCC model are based on reviews by Font-Palma et al. (2021) and Wang et al. (2013). In addition, the --- represents the theoretical minimum of 0.375 MJ/kg-CO₂ for CO₂ separation Berger et al. (2020).

It appears from Figure 4.7, that the CCC model presented in this report deviates with 16.9 % from the empirical CCC model. However, it also appears that the empirical CCC model does not take the refrigerant cycle of the contact liquid into account, which may be a contributing factor to the deviation between the mod-

elled CCC process and the empirical CCC model. However, since the majority of the heat required for the CCC model can be recovered internally in the process, it appears that the energy duty is relatively close to the theoretical minimum, compared to the other technologies. Consequently, the large potential for heat integration is crucial for the CCC technology in order to achieve the lowest possible energy duty. Furthermore, as stated previously, the CO₂ concentration in the off-gas is expected to have a major impact on the resulting energy duty. As a result, a sensitivity analysis of the modelled CCC process must be conducted in order to investigate the correlation between the energy duty and the CO₂ concentration in the off-gas.

4.5 Sensitivity Analysis of the CCC Model

The sensitivity analysis will be evaluated based on the energy-optimised CCC model with heat integration. It appears from section 4.3, that the CCC model could reach an energy duty of 0.89 MJ/kg-CO₂, based on a CO₂ concentration of 17.39 mol.%. Consequently, the correlation between the CO₂ concentration in the off-gas and energy duty will be investigated. The resulting correlation is presented in Figure 4.8 with the initial case of 0.89 MJ/kg-CO₂ with a corresponding CO₂ concentration of 17.39 mol.% marked with the arrow.

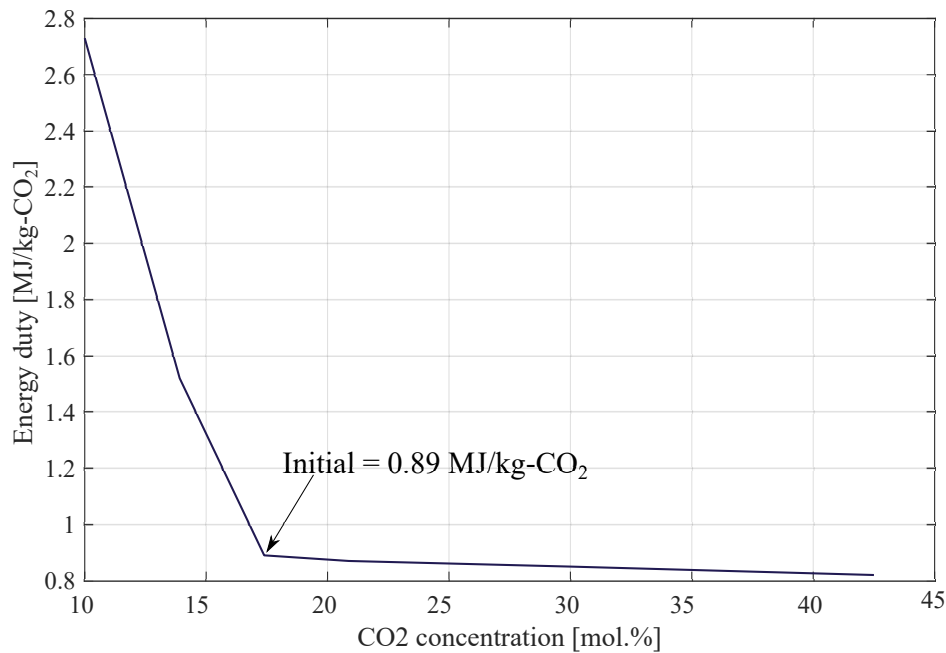


Figure 4.8: Energy duty of the CCC model as a function of the CO₂ concentration in the off-gas. The initial value of 0.89 MJ/kg-CO₂ based on the off-gas composition from Kær (2019) is marked with an arrow.

To evaluate the energy duty with respect to the the CO₂ concentration, the initial value of 17.4 mol.% has been varied with $\pm 20\%$ to a value of 20.9 and 13.9 mol.%, respectively. Besides, two outer points of 10 and 42.5 mol.% have been established. The resulting energy energy at the lower boundary is determined to 2.73 MJ/kg-CO₂, whereas the energy duty obtained at the higher boundary condition is 0.81 MJ/kg-CO₂. Due to the unambiguous trend, the incentive to further investigate the calcination and combustion process in order to increase the CO₂ concentration is clear. Consequently, a study of the calcination and combustion process will be conducted in order to identify the most significant parameters affecting the CO₂ concentration in the cement plant off-gas.

Chapter 5

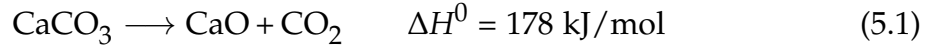
Technical Analysis of the Calcination and Combustion Process

Within this chapter, the calcination and combustion process will be modelled in Aspen Plus[®] to investigate the possibility of increasing the CO₂ concentration in the cement plant off-gas and simultaneously lowering the energy duty and increasing the capture potential. Subsequently, a sensitivity study of the combustion process will be conducted in order to identify the most influential parameters on the CO₂ concentration.

5.1 Development of the Calcination and Combustion Model

The dominating processes affecting the cement plant off-gas composition are the calcination and combustion process, as stated in Chapter 2, section 2.2. The CO₂ produced from the calcination process is assumed to be constant and solely temperature and pressure dependent. As a result, the combustion process is the only adjustable variable in order to increase the CO₂ concentration in the off-gas. To determine the fuel consumption required to force the calcination reaction, the energy consumption associated with the isothermal and isobaric calcination process must

be determined. The calcination process is modelled in Aspen Plus[®] based on an annual CaCO₃ consumption of 3,537,868 tonne/year at Aalborg Portland (Aalborg Portland A/S, 2019a). The calcination reaction is presented in (5.1).



Based on equation (5.1), the enthalpy of reaction for the calcination process can be determined to 178 kJ/mol-CaCO₃. Besides the enthalpy of reaction, a heat consumption associated with dissociation reactions must be taken into account. The heat consumption to cover the heating of the limestone from ambient temperature to the calcination temperature of 1,500 °C and the dissociation reactions are estimated to be 159.13 kJ/mol-CaCO₃, based on the Aspen Plus[®] model. However, due to the fact that the calcination in Aspen Plus[®] is considered adiabatic, an additional heat loss to the surroundings must be taken into account and is assumed to be 50.51 kJ/mol-CaCO₃ (Lin et al., 2011). Consequently, the total energy consumption is expected to be 387.64 kJ/mol-CaCO₃. Thus, the heat required for the calcination process can be determined by multiplying with the mole flow rate of the CaCO₃. The resulting energy consumption for the calcination process is approximately 434.1 MW.

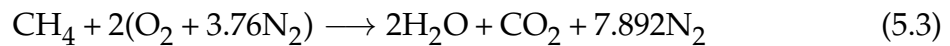
Based on the total energy consumption, the amount of fuel can be estimated using the lower heating value (LHV). The LHV is used as the latent heat from the vaporisation of the water is not recovered, and the water vapour from the combustion is released with the off-gas. Consequently, the general equation to estimate the mass flow rate of fuel for the combustion is presented in equation (5.2).

$$\dot{m}_{\text{fuel}} = \frac{\dot{Q}_{\text{tot,cal}}}{\text{LHV}_{\text{fuel}}} \quad (5.2)$$

The combustion model is assumed to be methane fired. Methane is utilised due to the fact that the captured CO₂ can be converted into methane through methanation and, in this way, be self-supplying. The energy requirement for the calcination process of 434.1 MW can be covered by an annual methane consumption of approximately 238,000 tonne/year, based on a LHV of 50 MJ/kg. Compared to the fuel consumption at Aalborg Portland of approximately 518,000 tonne/year

(Aalborg Portland A/S, 2019a), the methane consumption is significantly lower. However, considering the significantly higher LHV for methane compared to the average LHV at Aalborg Portland which is estimated to be 35 MJ/kg and the fact that the water content from the limestone supply is not taken into account, the estimated fuel consumption is considered reasonable.

Based on the assumption regarding a methane fired combustion, the corresponding air flow can be estimated using the Air to Fuel ratio (AFR), as presented in Appendix B, equation (B.7). The AFR is calculated based on the combustion reaction presented in equation (5.3).



For a methane fired combustion process, the stoichiometric AFR can be determined to be 17.16. The associated mass flow calculations as well as the AFR calculation are elaborated in Appendix B, section B.1. Based on the stoichiometric AFR and an assumed excess air coefficient, the mass flow of air can be determined. The excess air coefficient takes the mixing ability of the fuel and air into account. Since the mixing abilities of methane and air are great, an excess air coefficient of $\lambda = 1.05$ is assumed (T. Condra, Personal Communication, 21st April, 2022). In other words, it is assumed that 5 % more air had to be supplied than for a stoichiometric combustion. This is in huge contrast to a coal-fired combustion, where the mixing abilities are poor. Hence, the combustion will require a significant higher excess air coefficient to achieve a total combustion. The excess air coefficient must likewise ensure that a complete combustion is achieved to prevent traces of methane in the off-gas. Methane in the off-gas is very inappropriate as methane is a powerful greenhouse gas. Since the combustion process is an integrated part of the CCU process train, the excess oxygen from the electrolysis can be utilised internally in the system. By the use of pure oxygen instead of an air supply, the oxidiser flow can be lowered by 4.76 times, due to the fact that air only consists of 21 % oxygen. Consequently, oxyfuel combustion will require a significantly lower volume flow compared to air combustion. Additionally, the heating demand for the oxidiser is significantly less due to the reduced volume flow.

Based on the evaluation of the calcination and combustion process and the determination of the associated fuel and oxidiser requirements, the combined calcination and combustion process can be evaluated in Aspen Plus[®]. Hence, a conceptual illustration of the calcination process is presented in Figure 5.1.

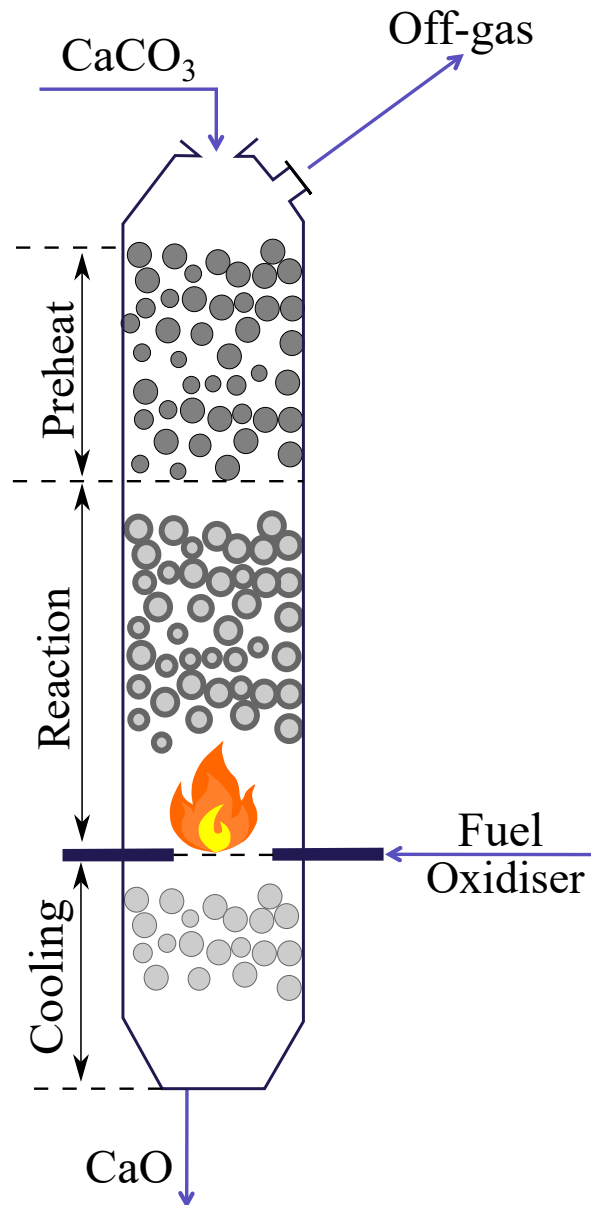


Figure 5.1: Conceptual illustration of the calcination and combustion process developed in Aspen Plus[®].

The resulting off-gas from the calcination and combustion process is based on isothermic and isobaric conditions. According to Aalborg Portland A/S (2019a) and Kær (2019), the calcination reaction occurs at 1,500 °C and 1 atm. However, since the calcination is evaluated based on a Gibbs reactor in Aspen Plus[®], the model cannot take the temperature gradient within the calciner into account.

The calcination process is assumed to be constant at isothermic and isobaric conditions. Thus, the changes in the off-gas volume flow and composition are solely affected by changes in the combustion process. However, as the methane consumption is determined based on the calcination reaction with dissociation, preheating of limestone and an estimated heat loss to the surroundings, the only variable is the oxidiser. The preheating of the oxidiser is neglected as it is expected to heat exchange with the CaO product leaving the calciner. However, air combustion will require significantly more preheating compared to oxyfuel combustion, as the volume flow is higher. However, this difference is not included in this calcination evaluation. The resulting off-gas compositions and molar flow from a calcination and combustion process with either air combustion or oxyfuel combustion are presented in Table 5.1.

Table 5.1: Off-gas comparison between the air combustion and oxyfuel combustion at isothermic and isobaric conditions extracted from Aspen Plus[®] model. The compositions are based on an average calcination temperature of 1,500 °C and pressure of 1 atm (Aalborg Portland A/S, 2019a).

Volume flow		
	Air	Oxyfuel
Volume flow [m ³ /h]	3.305·10 ⁶	1.352·10 ⁶
Composition		
Compounds [mol.%]	Air	Oxyfuel
Nitrogen	59.5	-
Water	15.02	37.1
CO ₂	24.6	60.8
Oxygen	0.773	1.97
Nitrogen oxide	0.0674	-
Nitrogen dioxide	3.239·10 ⁻⁵	-
CO	0.0428	0.0663
Hydrogen	7.138·10 ⁻³	0.0111

An oxyfuel combustion results in a 59.1 % lower volume flow compared to air combustion, as presented in Table 5.1. This difference can have a major impact on the sizing of the CCC technology, as carbon capture technologies typically are scaled with respect to the volume flow. It also appears that there are not traces of neither nitrogen nor NO_x, as it is assumed that the oxygen and CaCO₃ supply is 100 % pure. However, an air supply is expected unavoidable with the limestone, which forms the basis for thermal NO_x formation, which the CCC model must be able to handle. Furthermore, a significant increase in the CO₂ and water concentrations appears due to the fact that the oxygen molecules are more likely to react with C and H molecules when the nitrogen is removed.

It appears from Table 5.1 that the CO formation in oxyfuel combustion increases significantly compared to air combustion. However, according to the emission requirement of 1,500 ppm presented in Table 5.1, the CO concentration of 663 ppm is not critical. Conclusively, in accordance with the data presented in Table 2.2, oxyfuel combustion will be very beneficial to the CCC process. However, to determine

the impact of the increased oxygen supply to the combustion process, a sensitivity analysis of the combustion process is further investigated

5.2 Sensitivity Analysis of the Combustion Process

The results obtained from the calcination and combustion process presented in Table 5.1 are based on a constant calcination temperature and pressure of 1,500 °C and 1 atm, respectively. However, the calcination temperature will vary depending on how close to the flame of the combustion process the calcination reaction occurs. The temperature closest to the flame is the Adiabatic Flame Temperature (AFT). The AFT depends on several parameters including the fuel type, oxidiser, and amount of dissociation. To solely investigate the trends from a methane fired combustion process without considering the impact of the calcination reaction, a combustion model has been developed in Cantera, which is presented in Supplementary 3. Based on the combustion model, the correlation between the AFT and the oxygen content in the oxidiser can be determined and is presented in Figure 5.2. The oxygen content varies from air combustion at 21 % oxygen to oxyfuel combustion at 100 % oxygen.

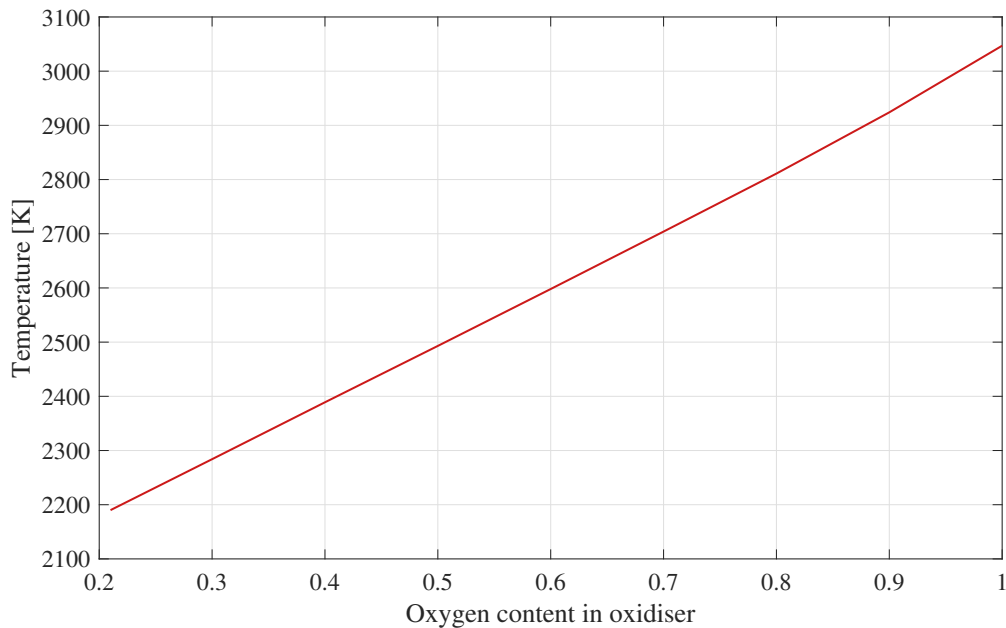


Figure 5.2: The adiabatic flame temperature of the combustion as a function of oxygen content in the oxidiser.

Figure 5.2 illustrates that the AFT is highly affected by changes in the oxygen content in the oxidiser. It appears that the AFT can reach approximately 3,040 K for oxyfuel combustion, which can result in major challenges for the material used in the rotary kiln. Subsequently, the increased AFT will likewise cause changes in the flue gas composition due to dissociation. The temperature-dependent behaviour of three of the most vital compounds is presented in Figure 5.3.

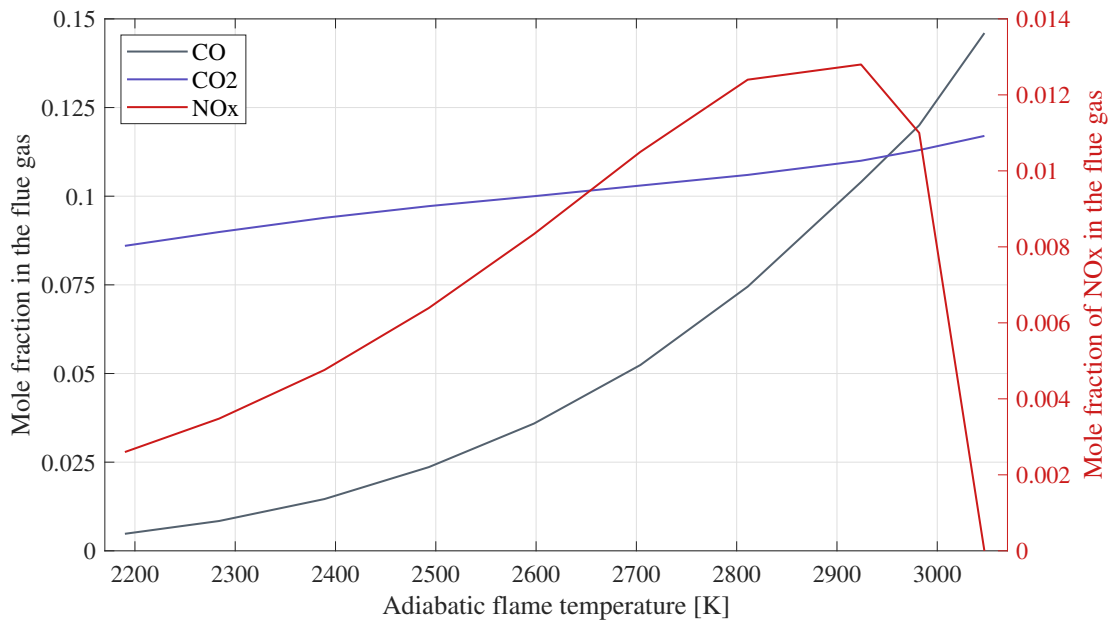


Figure 5.3: The mole fraction of CO and CO₂ in the flue gas on the left y-axis and the mole fraction of NO_x in the flue gas on the right y-axis as a function of the adiabatic flame temperature.

It appears from Figure 5.3 that an increased AFT will result in an increasing concentration of CO and CO₂. However, the CO formation will increase more significantly compared to the CO₂ formation, which can be explained by thermal displacement of the CO/CO₂ equilibrium. The increased CO content in the flue gas is very inappropriate due to the strict legislation limits presented in Table 2.2.

The resulting thermal NO_x formation following a change in AFT is likewise presented in Figure 5.3. The NO_x formation occurs due to the dissociation of nitrogen and oxygen. The significant decrease in the NO_x concentration after approximately 2,900 K is due to the fact that the nitrogen content in the oxidiser goes toward zero when the AFT approximates oxyfuel combustion. However, it appears from Figure 5.3 that independently of the combustion process, the NO_x concentration must be reduced to comply with the emission limits stated in Table 2.2.

In order to prevent an inappropriate high AFT for oxyfuel combustion, a subset of the flue gas can be recirculated. The impact of recirculation is investigated

in Supplementary 4. Consequently, the correlation between recirculation and the resulting AFT for oxyfuel combustion is presented in Figure 5.4. The recirculate is cooled to 100 °C prior to the reinjection (Granados et al., 2011). It appears from Figure 5.4 that even with 50 % recirculation, the resulting AFT will only be reduced to approximately 2,920 K, which is still considered as a critically high AFT. This indicates that oxyfuel combustion will require a significant amount of external cooling to protect the equipment and ensure that no inappropriate thermal CO and NO_x formation occurs. Furthermore, this also means that oxyfuel combustion cannot be considered a retrofit possibility as the technology will require that the entire cement plant should be redesigned.

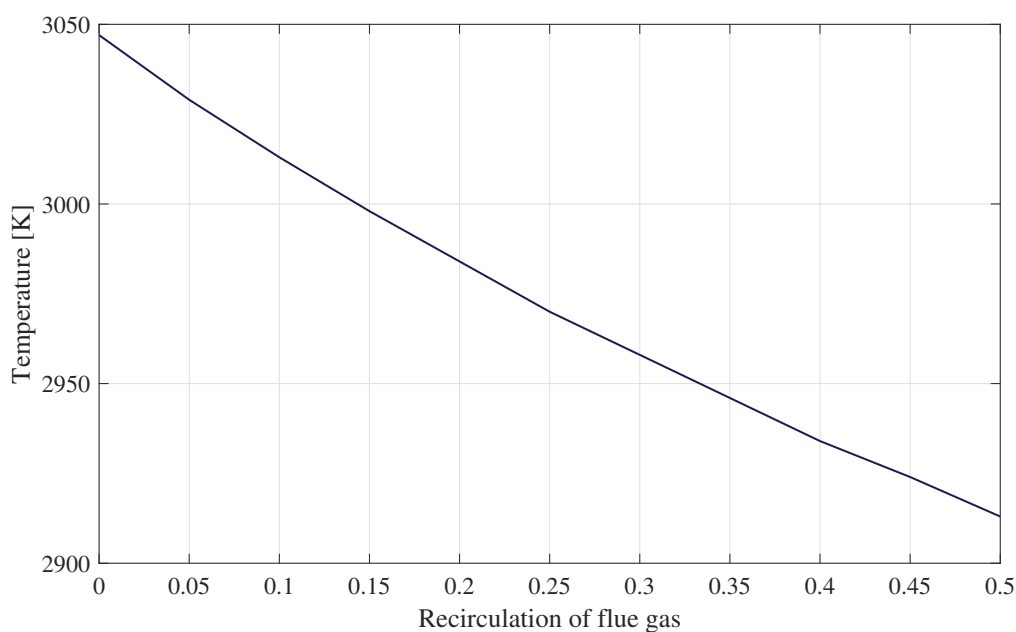


Figure 5.4: The adiabatic flame temperature based on oxyfuel combustion as a function of recirculation of the flue gas.

Furthermore, it appears from Figure 5.5 that the amount of recirculation has a major impact on the resulting flue gas composition. Specifically, the CO₂ concentration will increase at the expense of the CO concentration. However, despite the reduced CO concentration, it is still inappropriately high and will require additional treatment to comply with the emission requirements presented in Table 2.2.

Besides, it appears that the NO_x concentration drops significantly due to an increase in recirculation. Incidentally, the tendency for NO_x formation presented in Figure 5.5 is based on 90 % oxygen in oxidiser, as the NO_x concentration in oxy-fuel combustion will be zero. However, similar to the CO content, the NO_x content must be further reduced to comply with the emission limits for discharge to the environment as stated in Table 2.2.

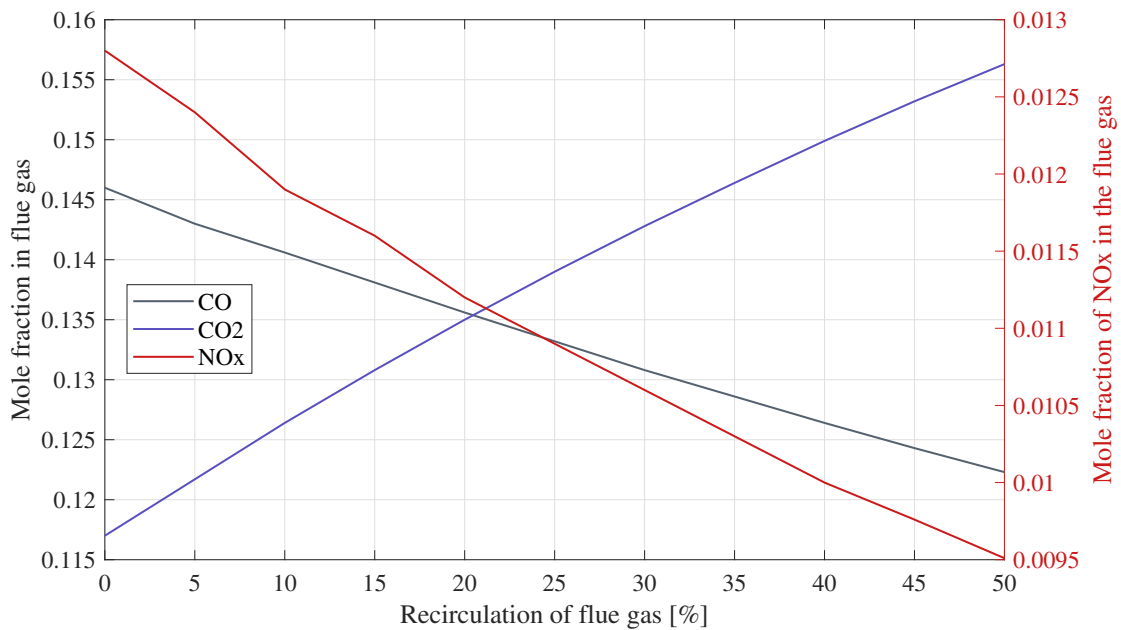


Figure 5.5: The resulting mole fraction of CO and CO₂ in the flue gas followed by an oxyfuel combustion as a function of recirculation. In addition, the mole fraction of NO_x in the flue gas is based on a 90 % oxygen content in the oxidiser is presented on the right y-axis.

Consequently, it appears from the sensitivity studies that the CO₂ concentration can be increased by increasing the oxygen content in the oxidiser or recirculating the flue gas. However, following the correlation between the oxygen content in the oxidiser and the AFT, the temperature might be a problem for the equipment used at the current cement plants. However, the increased oxygen content in the oxidiser also causes an inappropriate displacement in the CO/CO₂ equilibrium, as well as an undesirable thermal NO_x formation. It appears from the sensitivity study that recirculation is not sufficient to prevent an undesirable high CO formation and to obtain a permissible AFT. As a result, external cooling must be added

to obtain a sufficiently low AFT and a CO concentration complying with the emission limits. Conclusively, oxyfuel combustion is not recommended unless these challenges are solved.

Despite the challenges regarding oxyfuel combustion, an enhanced oxygen content in the oxidiser might be beneficial to the energy duty of the CCC process. In order to identify whether enhanced oxygen combustion is a possibility, a material-specific maximum AFT for the existing cement plant must be identified. In addition, the emission criteria for NO_x and CO must be complied with either with or without external purification. Finally, the maximum amount of recirculation and the recirculation temperature must be determined. Based on these plant specifications, the maximum oxygen content in the oxidiser can be determined. However, these practical specifications have not been collected. As a result, the maximum amount of oxygen concentration in the oxidiser cannot be determined.

Based on the evaluation of the calcination and combustion process, the oxyfuel combustion resulted in several inappropriate challenges, with which an air combustion is considered the most suitable for retrofitting. Furthermore, it appears that the CO₂ concentration in the cement plant off-gas can be increased by a methane fired combustion process, resulting in a reduced energy duty. In order to utilise the captured CO₂ and be self-supplying with methane, a Power to X (PtX) integration will be further investigated.

Chapter 6

Integration to Power to X Chain

Within this chapter, the Power to X (PtX) integration of the CCC model in order to produce methane to supply the calcination and combustion process will be investigated.

The PtX integration is modelled based on the CO₂ outlet stream from the CCC model presented in Table 4.2. The captured CO₂ can be utilised in several applications, as described in Chapter 2, section 2.1.1. In this report, the main focus is to utilise the captured CO₂ for methane production in order to supply the combustion process. As a result, a hydrogen supply for the methanation is required as expressed in equation (2.2). The total hydrogen demand required to convert the captured CO₂ from the CCC process into methane can be determined based on equation (6.1).

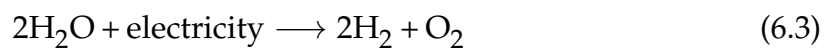


It appears from equation (6.1), that the methanation requires 4 moles of hydrogen per mole of CO₂ and is highly exothermic (S.Pieta et al., 2021). To force the CO₂ methanation, a nickel catalyst is commonly used. Additionally, the methanation commonly occurs in a temperature range of 249-449 °C. The upper limit of the temperature range should prevent an inappropriate formation of CO as a consequence of reverse water gas shift, presented in equation (6.2).



However, in a study conducted by S.Pieta et al. (2021), the highest methane yield is obtained at 349 °C resulting in a conversion rate of > 97 %.

In addition, it appears that the methanation reaction produces water, which can be used to cover a subset of the water demand for the electrolysis process. The electrolysis process is utilised to produce the hydrogen demand for the methanation reaction. Electrolysis is a cleavage process in which water is ionised into hydrogen and oxygen due to the presence of electricity. The electrolysis reaction is presented in equation (6.3).



It appears from equation (6.3) that the electrolysis produces oxygen, which might be utilised in the combustion process or an external application. The hydrogen production from the electrolysis is stated in Figure 6.1, based on the mass calculations presented in Appendix B, section B.2. Besides, the electrolysis process will act as a grid balancing technology, which can stabilise the grid by purchasing electricity during periods of low demand. As a result, surplus electricity can be used to produce hydrogen and hence contribute to methane production.

The resulting demand of hydrogen to cover the methanation is scaled with respect to the captured CO₂ as presented in Figure 6.1. Furthermore, the methanation is based on a total conversion rate of 100 % with regard to the captured CO₂. The mass flows presented in Figure 6.1 are elaborated in Appendix B, section B.2.

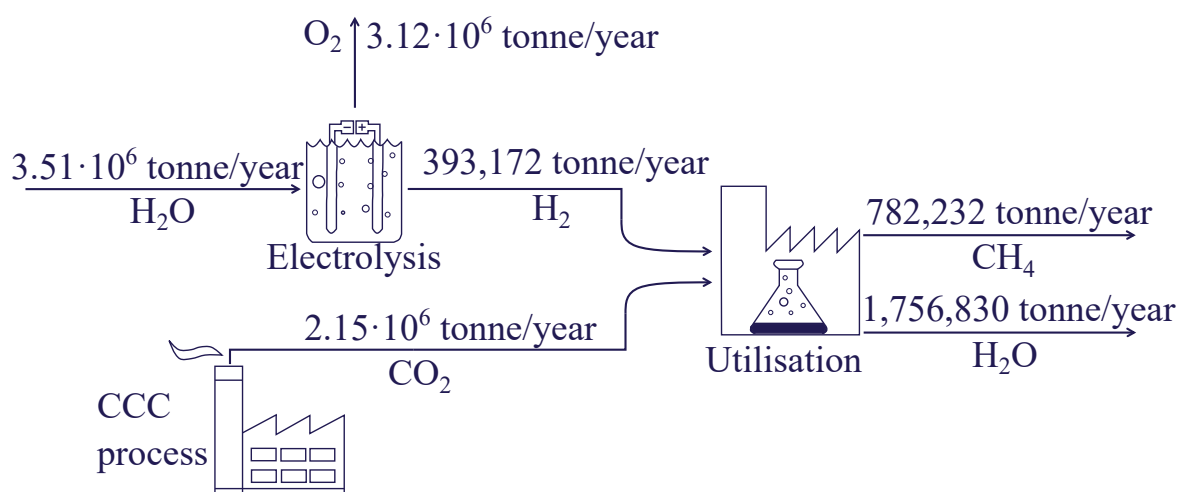


Figure 6.1: The associated mass flows of CO₂, hydrogen, oxygen, methane, and water scaled with respect to the CO₂ captured from the CCC model.

The hydrogen is expected to come from a low temperature alkaline electrolysis process as this technology is commercially utilised. According to Jensen (2017), the alkaline electrolysis process operates below 100 °C. The electricity consumption required per kg of hydrogen is estimated based on a cell efficiency of $\eta = 64.5$ %, the enthalpy of formation for water, and the molar flow of hydrogen needed to make a total conversion of the captured CO₂ (Sarkar and Bhattacharyya, 2012). Since the electrolysis reaction converts water into hydrogen and oxygen, it will only be the enthalpy of formation for water that is included since all pure elements have an enthalpy of formation of 0. Consequently, the electricity consumption for the electrolysis process is calculated solely based on water's enthalpy of formation with the corresponding cell efficiency. The resulting electricity consumption amounts to 60.91 kWh/kg of hydrogen.

One of the challenges of producing hydrogen from electrolysis is the large water consumption. A minimum of approximately 9 kg of water must be used to produce 1 kg of hydrogen. Furthermore, the current state of the art uses drinking water as the electrolysis is unable to use seawater (Tong et al., 2020). However, the use of drinking water poses an ethical issue, as drinking water is not considered as a renewable resource. As a result, desalination and demineralisation of seawater

could make the technology more sustainable. However, desalination and demineralisation will result in significantly higher energy consumption for the process (Lampert et al., 2016).

Based on the hydrogen consumption stated in Figure 6.1 and the electricity demand of 60.91 kWh/kg-H₂, the corresponding electricity consumption can be estimated to 2,806 MW for the electrolysis process. Conclusively, the three models considering the CCC process, the combustion and calcination process, and the PtX integration will, in combination, form the basis of an overall system evaluation.

Chapter 7

Evaluation of the Process Train

In this chapter, an overall evaluation of the process train will be conducted. Hence, the combined methane fired combustion and calcination process will be connected to the CCC process prior to the methanation process. Additionally, the evaluation will embrace the mass balances between the different processes and the resulting energy consumption. The evaluation will consist of two cases, consisting of a total methane conversion and exclusively self-supplying methane conversion. Finally, the capability of direct air capture will be investigated for the CCC model.

The mass Sankey diagram of the process train with total methane conversion is outlined in Figure 7.1. The CaCO_3 supply to the calcination process is relative to the supply at Aalborg Portland, while the remaining stream specifications are based on modelled data extracted from Aspen Plus[®].

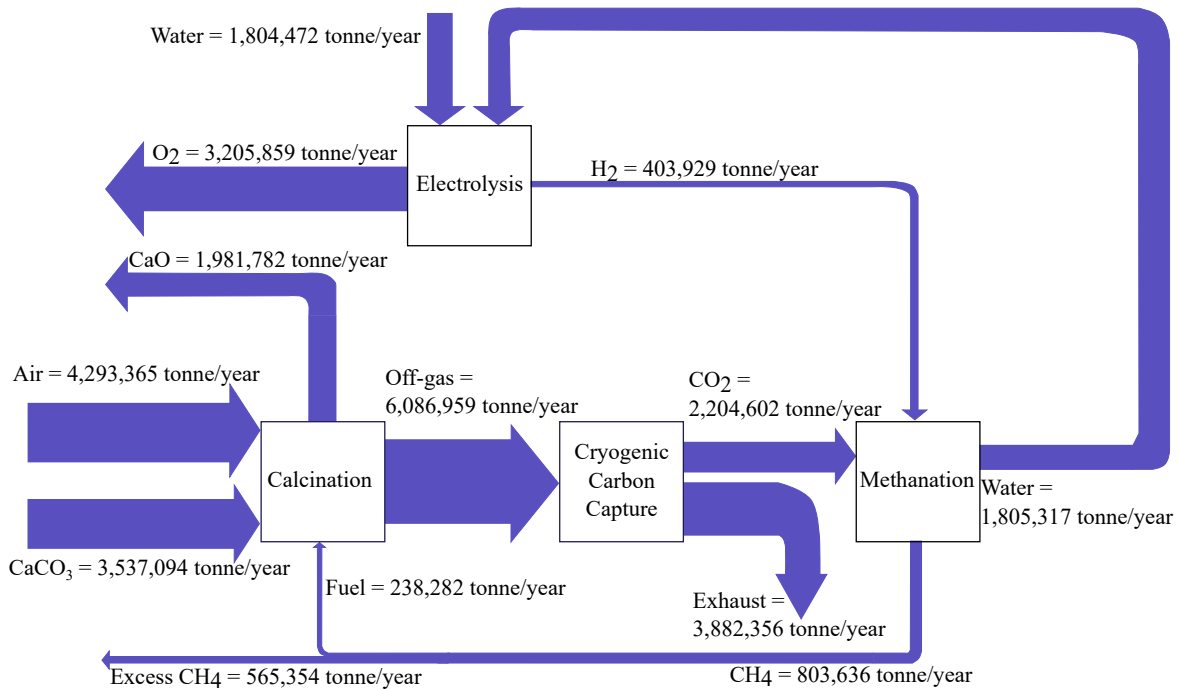


Figure 7.1: Mass-based Sankey diagram of the process train representing a total methane conversion. The mass flows are scaled with respect to the calcination off-gas.

It appears from Figure 7.1 that a large amount of surplus oxygen is available from the electrolysis process. Consequently, this surplus oxygen must be utilised either to enhanced oxygen combustion or stored prior to further utilisation in an external application. Furthermore, an exhaust gas is likewise discharged from the CCC process. Dependent on the calcination and combustion process, this exhaust gas might require additional treatment in order to comply with the emission limits stated in Table 2.2. However, based on an air combustion and an average calcination temperature of 1,500 °C, the corresponding exhaust gas will only require NO_x treatment before discharge.

Conclusively, it appears from Figure 7.1, that if the entire amount of captured CO₂ is converted into methane, it will result in excess methane, which must be used in external applications. However, Denmark has a very well-distributed natural gas grid, where surplus methane can be supplied and generate an additional income.

Furthermore, an associated energy evaluation of the processes can be conducted based on the resulting mass balances. The energy evaluation of the processes considering a total methane conversion is presented in Table 7.1. In addition, the energy consumption of the electrolysis and the methanation processes do not consider the potential of heat integration, by which the energy consumption might be further reduced. The energy consumption is determined based on the energy duties and the corresponding mass flows of CO₂, hydrogen, and methane presented in Figure 7.1. Furthermore, the energy consumption associated with the CCC process and the electrolysis process are power consuming, while energy consumption of the methanation solely requires thermal energy.

Table 7.1: Energy evaluation of the total methane conversion based on the post calcination processes.

Energy evaluation of the total methane conversion		
Process	Energy duty	Energy consumption
Cryogenic carbon capture	0.85 MJ/kg-CO ₂	59.38 MW
Electrolysis	219.26 MJ/kg-H ₂	2,802.11 MW
Methanation	51.43 MJ/kg-CH ₄	1,309.73 MW
Total energy consumption		4,171.22 MW

Based on the energy evaluation, it is clear that the electrolysis process is the largest consumer with 2,802.11 MW. By summarising the three contributions, the total energy consumption can be determined to be 4,171.22 MW. Conclusively, it appears that the energy consumption from the CCC process can be considered negligible compared to the electrolysis and methanation processes. Since methane production is by far the largest energy consumer, an alternative case can be considered. In this case, the energy consumption is evaluated based on a methane production that solely cover the demand from the calcination and combustion process. Consequently, the largest energy-consuming processes should solely ensure that the calcination and combustion process remains self-supplying. The resulting mass-based Sankey diagram is presented in Figure 7.2. It appears from Figure 7.2 that only a subset of the CO₂ is chemically converted into methane, following the limited methane production. Consequently, the remaining captured CO₂ must be

either utilised in an external process or stored.

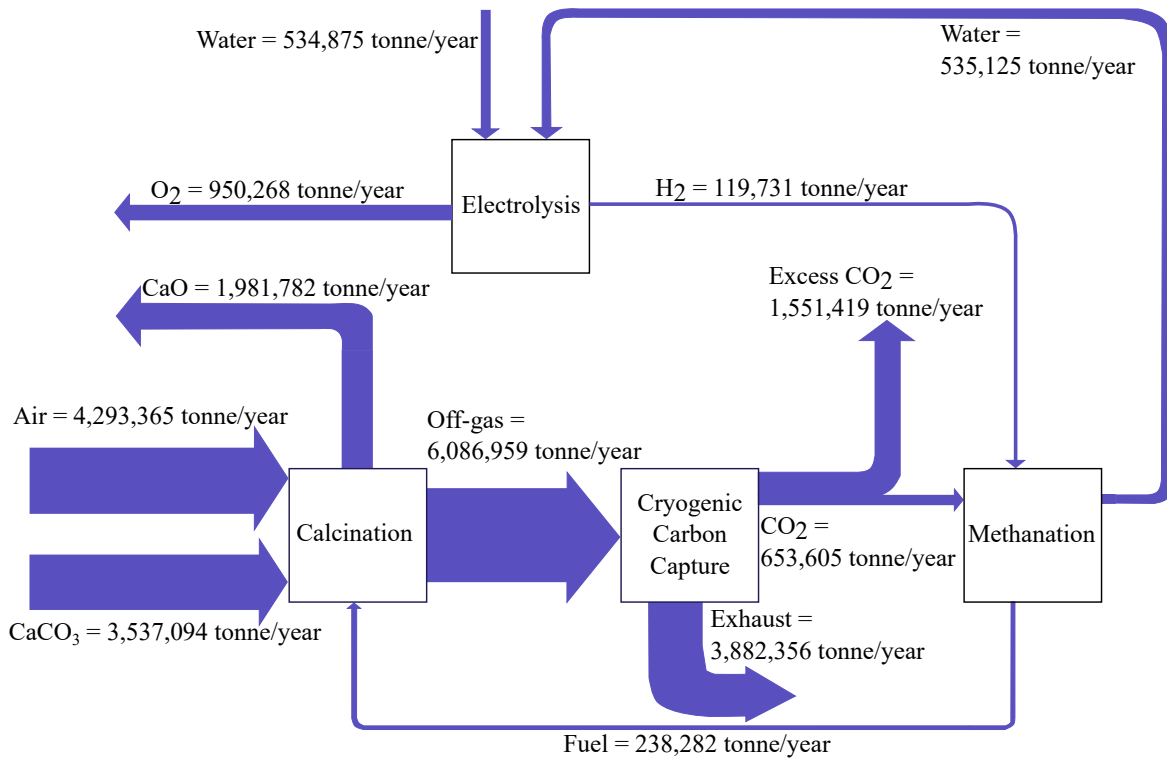


Figure 7.2: Mass-based Sankey diagram of the self-supplying process train, scaled with respect to the calcination off-gas.

By considering the newly obtained mass flows, the resulting energy consumption can be determined. The energy duties for the processes will remain constant, due to the fact that they are considered independent of the scale. The resulting energy consumption of the processes are presented in Table 7.2. Compared to the energy consumption of the process train considering a total CO_2 methanation, the electrolysis process is reduced to 831.90 MW, which is a decrease of 70.3 %. Similarly, the energy consumption of the methanation is reduced by 70.4 % resulting in energy consumption of 388.34 MW. In combination, the exclusively self-supplying process train results in a total energy consumption of 1,279.63 MW, resulting in a total reduction of 69.3 %.

Table 7.2: Energy evaluation of the self-supplying process train based on the post calcination processes.

Energy evaluation of the self-supplying process train		
Process	Energy duty	Energy consumption
Cryogenic carbon capture	0.85 MJ/kg-CO ₂	59.38 MW
Electrolysis	219.26 MJ/kg-H ₂	831.90 MW
Methanation	51.43 MJ/kg-CH ₄	388.34 MW
Total energy consumption		1,279.63 MW

Conclusively, the exclusively self-supplying process train will lower the energy consumption significantly. However, the overall evaluation of the profitability is dependent on the potential income of the excess methane, compared to the disposal cost of the excess CO₂. As a result, an economic evaluation must be developed in order to determine the most profitable solution.

7.1 Direct Air Capture Ability

In the modelling of the CCC process in combination with a cement production, the air supply to the combustion process is assumed to be a binary mixture between nitrogen and oxygen. However, other components, such as 380 ppm CO₂, also appear in the ambient air (de la Vega et al., 2020). As the CCC process achieves a CO₂ recovery of 99.97 %, it makes sense to include this subset of CO₂ in the air supply to investigate the possibility of Direct Air Capture (DAC). It appears from the model that by including 380 ppm of CO₂ in the airflow, the resulting CO₂ capture will increase with 285.9 kg/hour, which is equivalent to an annual increase in CO₂ capture of 2,507 tonne/year. This is significantly more than the annual CO₂ loss through the exhaust gas and the bleed, which combined amount to 11 tonne/year. Conclusively, the CCC process can be categorised as a DAC technology, which annually removes 2,496 tonne/year of CO₂ from the atmosphere. As a result, the entire process can be considered CO₂ negative as the process captures more CO₂ than it emits. The difference between the CO₂ content in the off-gas and the deviation in the amount of captured CO₂, with and without considering the

CO₂ content in the air, is presented in Table 7.3.

Table 7.3: Evaluation of the CO₂ mass flow from the off-gas and the resulting captured CO₂ stream, with and without CO₂ content in the air supply.

Evaluation of the CO₂ flow from the off-gas and the resulting captured CO₂ stream		
	Air supply without CO₂	Air supply with CO₂
CO ₂ content in the off-gas [tonne/year]	2,205,089	2,207,599
Captured CO ₂ stream [tonne/year]	2,204,554	2,207,061

Moreover, by increasing the amount of captured CO₂, the corresponding energy duty will also be reduced. As a result, by including the CO₂ content in the air-flow to the methane fired combustion process, the energy duty for the CCC process will be reduced from 0.85 MJ/kg-CO₂ to 0.849 MJ/kg-CO₂. Consequently, the CCC process can capture CO₂ directly from the air to an energy duty of 0.849 MJ/ kg-CO₂, which is significantly lower compared to conventional DAC technologies, which use approximately 7.2 MJ/kg-CO₂ (Lebling and Leslie-Bole, 2022). However, the CCC technology cannot be considered a standalone DAC solution since it requires a point source in order to achieve a remarkable energy duty.

Chapter 8

Conclusion

Throughout this study, a technical evaluation of the Cryogenic Carbon Capture (CCC) process and the opportunity for a Power to X integration has been performed in order to answer the following thesis statement:

Is cryogenic solid-vapour separation a suitable carbon capture technology for a cement plant off-gas in view of the technical potential, and is it possible to achieve synergistic effects between the cement production, the carbon capture technology, and the PtX integration?

Specifically, a model of the CCC process has been developed to investigate the possibility of obtaining a purified CO₂ stream which complies with the requirements for methane production. The CCC process model is scaled with respect to the off-gas composition and mass flow discharged from Aalborg Portland of 8,337,970 tonne/year. In addition, a model of the calcination and combustion process as well as the methanation with an adjacent electrolysis process has been developed. These models are developed in order to investigate the suitability of the CCC process in combination with a PtX utilisation facility.

The modelled calcination process is scaled with respect to the annual CaCO₃ consumption at Aalborg Portland. The associated combustion process is assumed to be methane fired due to the favourable lower heating value. By considering a

methane fired combustion process, the fuel can be produced on-site by methanation, resulting in a self-supplying process train. The resulting methanation process with corresponding electrolysis capacity is initially scaled in order to achieve a total methane conversion of the captured CO₂ from the CCC model.

The models have been developed in Aspen Plus[®] and Cantera. The results from the CCC model showed that a CO₂ recovery of 99.9 % with a corresponding purity of 99.96 mol.% could be obtained. As a result, the CO₂ purity requirement for methanation is met. Subsequently, the CCC model has been optimised in order to lower the energy duty per kg of captured CO₂. Conclusively, the energy optimisation resulted in an energy duty of 5.77 MJ/kg-CO₂. However, by considering the possibility of heat integration, the energy duty could be further reduced by 84.6 %, resulting in an energy duty of 0.89 MJ/kg-CO₂.

Subsequently, a sensitivity analysis of the CCC model has been conducted to investigate the correlation between the CO₂ concentration in the cement plant off-gas and the resulting energy duty. The analysis showed that by increasing the CO₂ concentration in the off-gas, the resulting energy duty will be reduced. Consequently, a sensitivity study of the combustion process has shown the possibility to increase the CO₂ concentration by adjusting the oxygen content in the oxidiser. Besides, the study showed a strong correlation between the adiabatic flame temperature and the oxygen content in the oxidiser. Furthermore, it appears that the off-gas composition is strongly correlated with the adiabatic flame temperature. Consequently, the oxyfuel combustion process was disregarded due to the inappropriate high adiabatic flame temperature as well as the resulting undesired concentrations of CO and NO_x. Conclusively, oxyfuel combustion is not recommended unless these challenges are solved.

By considering the methane fired calcination and combustion process, the CO₂ concentration in the off-gas is increased, resulting in an energy duty of 0.85 MJ/kg-CO₂. In Figure 8.1, the resulting energy duties for the two CCC models are compared to an empirical CCC model and other conventional separation technologies.

The initial CCC model is approximated with an off-gas composition inspired by Kær (2019), while the CCC model* is evaluated based on the modelled methane fired calcination and combustion process. In addition, all the CO₂ separation technologies are compared to a theoretical minimum energy duty, which is estimated to be 0.375 MJ/kg-CO₂ (Berger et al., 2020).

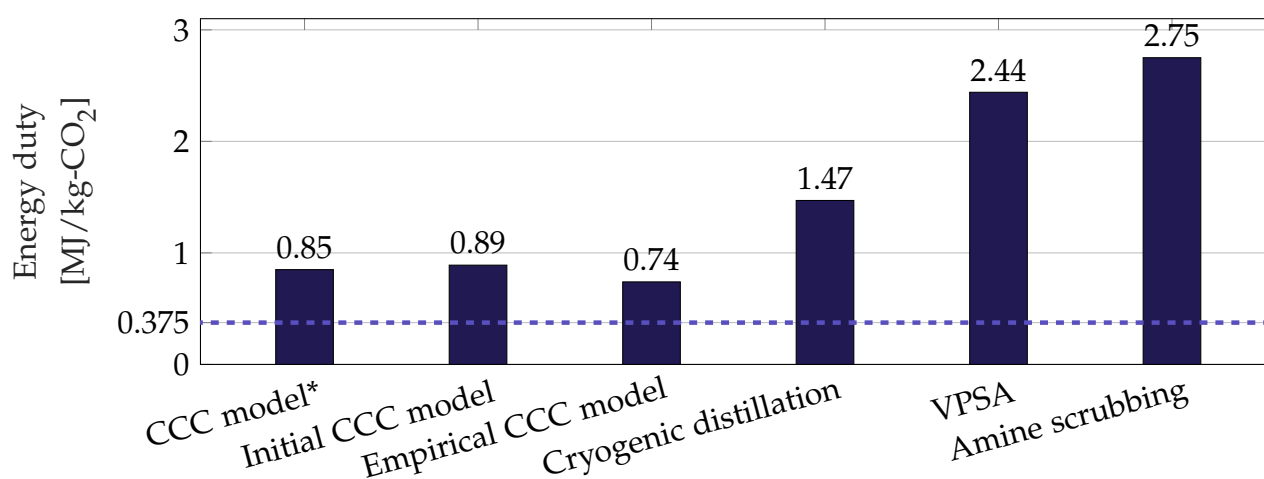


Figure 8.1: Comparison of the energy duties between the two developed CCC models and the carbon capture technologies described in Chapter 2. The energy duties of the technologies besides the developed CCC models are based on reviews by Font-Palma et al. (2021) and Wang et al. (2013). The CCC model* is based on a off-gas from a modelled calcination process with a methane fired combustion. In addition, the - - - represents the theoretical minimum of 0.375 MJ/kg-CO₂ for CO₂ separation.

Finally, an evaluation of the entire process train including the calcination and combustion process, the optimised CCC process, and the methanation with associated electrolysis process is conducted. The evaluation is divided into two cases, a total methane conversion and an exclusively self-supplying methanation process. Both evaluations showed that the electrolysis process is the most energy-consuming process, resulting in an energy consumption of 2,802.11 MW for the total methane conversion and 831.90 MW for the exclusively self-supplying methane conversion. Conclusively, the total energy consumption of the two cases is determined to be 4,171.22 MW and 1,279.63 MW for total methane conversion and exclusively self-supplying methane conversion, respectively. However, it will require economic

considerations to determine which of the two cases is the most profitable solution. This is due to the fact that the valuation of a surplus methane production must be taken into account, as well as the potential disposal costs associated with a surplus CO₂ stream. However, by considering the two cases solely based on the energy consumption, the exclusively self-supplying methane production will result in the lowest accumulated energy consumption.

Furthermore, by including CO₂ content in the airflow used as the oxidiser to the calcination and combustion process, the annual amount of captured CO₂ in the CCC process increases by 2,496 tonne/year. Additionally, by considering the direct air capture ability, the resulting energy duty of the CCC process can be slightly decreased to 0.849 MJ/kg-CO₂. Conclusively, the cement production in combination with the CCC process can be considered CO₂ negative.

8.1 Recommendations for Future Studies

The conclusions obtained in this report are based on several assumptions which must be further investigated to support the results. First and foremost, the desublimation column and the melter in the CCC model are simplified with Gibbs reactors to approximate the thermodynamic behaviour. In particular, the desublimation process is modelled based on a single Gibbs reactor, which means that the temperature is assumed to be constant during the solidification. To make a better approximation, it will require several Gibbs reactors to incorporate the consequences of a temperature gradient within the desublimation column. Furthermore, the CCC model must be investigated from an experimental point of view to investigate whether there are factual challenges that are not taken into account in the CCC model.

Additionally, the pressure losses in the pipes and heat exchanges must be considered as it has been disregarded in the CCC model. By including the pressure losses, the energy consumption related to the pressure-changing components will be higher than currently expected, which must be taken into account to determine the actual energy consumption.

Additionally, the water content extracted from the off-gas in the dryer component will most likely contain dissolved impurities and need treatment to comply with the emission limits. Consequently, the impact of the minor components disregarded from the off-gas composition should be investigated to determine the amount of post-treatment required prior to discharge to the environment.

In addition, it appears that the electrolysis process requires heating to force the ionisation of water to produce hydrogen and oxygen. In contrast, methanation requires cooling to maintain the desired operating temperature in order to achieve the highest possible conversion rate. Consequently, by implementing heat integration between these processes, the total energy demand will be reduced.

Furthermore, in general it will be evident to investigate a plant-based heat integration to reduce the total heat demand for the entire process train. In this way, any hot or cold utilities can be utilised internally to reduce the total heat demand for the system.

Finally, the raw material used for the calcination process is pure CaCO_3 . Compared to the raw material used at Aalborg Portland, a significant amount of water has been disregarded. This must be considered due to the high energy consumption for heating and evaporating, which will result in a significantly higher methane consumption. Consequently, it will require an equivalent amount of water to benchmark the methane consumption in this report with the fuel consumption at Aalborg Portland.

References

- Aalborg Portland A/S. Aalborg Portland Environmental Report 2019. Environment and Health & Safety. Technical report, Aalborg Portland A/S, 2019a. URL www.aalborgportland.dk. https://www.aalborgportland.dk/wp-content/uploads/2020/10/Aalborg_Portland_Environmental_Report_2019_web.pdf.
- Aalborg Portland A/S. GRØNT REGNSKAB OG ARBEJDSMILJØ. Technical report, Aalborg Portland A/S, 2019b.
- D. Aaron and C. Tsouris. Separation of CO₂ from flue gas: A review. *Separation Science and Technology*, 40(1-3):321–348, 2005. ISSN 01496395. doi: 10.1081/SS-200042244. URL <https://www.tandfonline.com/doi/abs/10.1081/SS-200042244>.
- V. Alvarado and E. Manrique. Enhanced oil recovery: An update review, 8 2010. ISSN 19961073. URL <https://www.mdpi.com/1996-1073/3/9/1529/html><https://www.mdpi.com/1996-1073/3/9/1529>.
- AspenTech. Aspen Plus ® User Guide. Technical report, Aspen Technology, Inc., 2000.
- AspenTech. Part Number : Aspen Physical Property System 11. *Engineering*, pages 2–18, 2001. URL <http://www.aspentech.com>.
- L. Baxter, C. Hoeger, K. Stitt, S. Burt, and A. Baxter. Cryogenic Carbon Capture™ (CCC) Status Report. *SSRN Electronic Journal*, 2021. doi: 10.2139/ssrn.3819906. URL <https://ssrn.com/abstract=3819906>.
- E. Benhelal, E. Shamsaei, and M. I. Rashid. Challenges against CO₂ abatement strategies in cement industry: A review, 6 2021. ISSN 18787320.

- A. H. Berger, C. Hoeger, L. Baxter, and A. Bhowan. Evaluation of Cryogenic Systems for Post Combustion CO₂ Capture. *SSRN Electronic Journal*, 1(October):1–8, 2020. doi: 10.2139/ssrn.3365753.
- A. Bosoaga, O. Masek, and J. E. Oakey. CO₂ Capture Technologies for Cement Industry. *Energy Procedia*, 1(1):133–140, 2 2009. ISSN 18766102. doi: 10.1016/j.egypro.2009.01.020.
- P. A. Brownsort. Briefing on carbon dioxide specifications for transport. 1st Report of the Thematic Working Group on: CO₂ transport , storage and networks. Technical Report November, EU CCUS PROJECTS NETWORK, 2019. URL <http://www.ccusnetwork.eu/>.
- R. Chauvy, N. Meunier, D. Thomas, and G. De Weireld. Selecting emerging CO₂ utilization products for short- to mid-term deployment. *Applied Energy*, 236: 662–680, 2 2019. ISSN 03062619. doi: 10.1016/j.apenergy.2018.11.096.
- COWI. Aalborg portland looks into possibilities of carbon capture, 2020. URL <https://www.cowi.com/about/news-and-press/aalborg-portland-looks-into-possibilities-of-carbon-capture>.
- E. de la Vega, T. B. Chalk, P. A. Wilson, R. P. Bysani, and G. L. Foster. Atmospheric CO₂ during the Mid-Piacenzian Warm Period and the M2 glaciation. *Scientific Reports*, 10(1), 12 2020. ISSN 20452322. doi: 10.1038/s41598-020-67154-8.
- I. Dincer and C. Zamfirescu. Conventional Power Generating Systems. In *Advanced Power Generation Systems*, pages 199–310. Elsevier, 1 2014. ISBN 978-0-12-383860-5. doi: 10.1016/b978-0-12-383860-5.00005-5.
- B. Dutcher, M. Fan, and A. G. Russell. Amine-based CO₂ capture technology development from the beginning of 2013-A review. *ACS Applied Materials and Interfaces*, 7(4):2137–2148, 2 2015. ISSN 19448252. doi: 10.1021/am507465f. URL <https://pubs.acs.org/doi/abs/10.1021/am507465f>.
- R. Dzurňák, A. Varga, J. Kizek, G. Jablonský, and L. Lukáč. Influence of burner nozzle parameters analysis on the aluminium melting process. *Applied Sciences*

- (*Switzerland*), 9(8):1614, 4 2019. ISSN 20763417. doi: 10.3390/app9081614. URL <https://www.mdpi.com/2076-3417/9/8/1614/html><https://www.mdpi.com/2076-3417/9/8/1614>.
- R. Dzurňák, A. Varga, G. Jablonský, M. Variny, M. Pástor, and L. Lukáč. Analyzing the formation of gaseous emissions during aluminum melting process with utilization of oxygen-enhanced combustion. *Metals*, 11(2):1–21, 2 2021. ISSN 20754701. doi: 10.3390/met11020242. URL <https://www.mdpi.com/2075-4701/11/2/242/html><https://www.mdpi.com/2075-4701/11/2/242>.
- Energistyrelsen. Dansk klimapolitik, 2020. URL <https://ens.dk/ansvarsomraader/energi-klimapolitik/fakta-om-dansk-energi-klimapolitik/dansk-klimapolitik>.
- Energistyrelsen. Punktkilder til CO₂ – potentialer for CCS og CCU Hovedkonklusioner, 2021. URL www.ens.dk.
- J. Farfan, M. Fasihi, and C. Breyer. Trends in the global cement industry and opportunities for long-term sustainable CCU potential for Power-to-X. *Journal of Cleaner Production*, 217:821–835, 4 2019. ISSN 09596526. doi: 10.1016/j.jclepro.2019.01.226.
- C. Font-Palma, D. Cann, and C. Udemu. Review of Cryogenic Carbon Capture Innovations and Their Potential Applications. *C*, 7(3):58, 2021. ISSN 2311-5629. doi: 10.3390/c7030058.
- S. O. Gardarsdottir, E. De Lena, M. Romano, S. Roussanaly, M. Voldsund, J. F. Pérez-Calvo, D. Berstad, C. Fu, R. Anantharaman, D. Sutter, M. Gazzani, M. Mazzotti, and G. Cinti. Comparison of technologies for CO₂ capture from cement production—Part 2: Cost analysis. *Energies*, 12(3):542, 2 2019. ISSN 19961073. doi: 10.3390/en12030542. URL <https://www.mdpi.com/1996-1073/12/3/542/html><https://www.mdpi.com/1996-1073/12/3/542>.
- I. Ghiat and T. Al-Ansari. A review of carbon capture and utilisation as a CO₂ abatement opportunity within the EWF nexus, 3 2021. ISSN 22129820.

- S. R. Gislason, D. Wolff-Boenisch, A. Stefansson, E. H. Oelkers, E. Gunnlaugsson, H. Sigurdardottir, B. Sigfusson, W. S. Broecker, J. M. Matter, M. Stute, G. Axelsson, and T. Fridriksson. Mineral sequestration of carbon dioxide in basalt: A pre-injection overview of the CarbFix project. *International Journal of Greenhouse Gas Control*, 4(3):537–545, 2010. ISSN 17505836. doi: 10.1016/j.ijggc.2009.11.013.
- D. Granados, J. Mejía, F. Chejne, C. Gomez, A. Berrío, and W. Jurado. Numerical Simulation of Oxy-Fuel Combustion in a Cement Kiln. *International Conference on Energy Process Engineering (ICEPE)*, 1(September 2015):184–187, 2011. URL www.ICEPE2011.de.
- D. E. Group. Clinker Calcination, 2020. URL <https://datis-inc.com/blog/clinker-calcination/>.
- T. Hills, D. Leeson, N. Florin, and P. Fennell. Carbon Capture in the Cement Industry: Technologies, Progress, and Retrofitting. *Environmental Science and Technology*, 50(1):368–377, 1 2016. ISSN 15205851. doi: 10.1021/acs.est.5b03508. URL <https://pubs.acs.org/doi/full/10.1021/acs.est.5b03508>.
- K. Hoyer, C. Hulteberg, M. Svensson, J. J. And, and O. Noerregaard. Biogas Upgrading-Technical Review, 2016. URL www.energiforsk.se.
- IEA. About CCUS, 2021. URL <https://www.iea.org/reports/about-ccus>.
- IECM. IECM Technical Documentation: Amine-based Post-Combustion CO₂ Capture. Technical report, Department of Engineering and Public Policy Carnegie Mellon University, 2018. URL www.iecm-online.com.
- J. O. Jensen. Low Temperature Electrolysis, 2017. URL <https://www.energy.dtu.dk/english/Research/Electrolysis-Cells/LT-Electrolysis>.
- M. Jensen. Energy Process Enabled by Cryogenic Carbon Capture. *BYU ScholarsArchive*, 2015. URL <https://scholarsarchive.byu.edu/etd>.
- S. K. Kær. C3U, Cryogenic Carbon Capture and Use. Technical report, Department of Energy Technology, 2019.

- M. Kozak, D. Wawrzyńczak, and I. Majchrzak-Kucęba. Separation and Recovery of Co₂ From Flue Gas Derived From the Cement Industry Sector : Vacuum Pressure Swing Adsorption research, 2017. URL <https://www.researchgate.net/publication/316717025>.
- A. Y. Ku, P. J. Cook, P. Hao, X. Li, J. P. Lemmon, T. Lockwood, N. M. Dowell, S. P. Singh, N. Wei, and W. Xu. Cross-regional drivers for CCUS deployment. *Clean Energy*, 4(3):202–232, 10 2020. ISSN 2515396X. doi: 10.1093/ce/zkaa008. URL <https://academic.oup.com/ce/article/4/3/202/5868404>.
- D. J. Lampert, H. Cai, and A. Elgowainy. Wells to wheels: Water consumption for transportation fuels in the United States. *Energy and Environmental Science*, 9(3): 787–802, 3 2016. ISSN 17545706. doi: 10.1039/c5ee03254g.
- K. Lebling and H. Leslie-Bole. Direct Air Capture: 6 Things To Know | World Resources Institute, 2022. URL <https://www.wri.org/insights/direct-air-capture-resource-considerations-and-costs-carbon-removal>.
- S. Lin, T. Kiga, Y. Wang, and K. Nakayama. Energy analysis of CaCO₃ calcination with CO₂ capture. *Energy Procedia*, 4:356–361, 2011. ISSN 18766102. doi: 10.1016/j.egypro.2011.01.062. URL <http://dx.doi.org/10.1016/j.egypro.2011.01.062>.
- A. Mathisen, H. Sørensen, N. Eldrup, R. Skagestad, M. Melaaen, and G. I. Müller. Cost optimised CO₂ capture from aluminium production. In *Energy Procedia*, volume 51, pages 184–190. Elsevier Ltd, 2014. doi: 10.1016/j.egypro.2014.07.021.
- J. M. Matter, M. Stute, S. Snæbjörnsdóttir, E. H. Oelkers, S. R. Gislason, E. S. Aradóttir, B. Sigfusson, I. Gunnarsson, H. Sigurdardóttir, E. Gunnlaugsson, G. Axelsson, H. A. Alfredsson, D. Wolff-Boenisch, K. Mesfin, D. F. D. L. R. Taya, J. Hall, K. Dideriksen, and W. S. Broecker. Rapid carbon mineralization for permanent disposal of anthropogenic carbon dioxide emissions. *Science*, 352 (6291):1312–1314, 6 2016. ISSN 10959203. doi: 10.1126/science.aad8132. URL <https://www.science.org/doi/abs/10.1126/science.aad8132>.

- L. A. Pellegrini. Process for the removal of CO₂ from acid gas, 2014. URL <https://www.freepatentsonline.com/9945605.html>.
- A. B. Rao and E. S. Rubin. A technical, economic, and environmental assessment of amine-based CO₂ capture technology for power plant greenhouse gas control. *Environmental Science and Technology*, 36(20):4467–4475, 10 2002. ISSN 0013936X. doi: 10.1021/es0158861. URL <https://pubs.acs.org/doi/abs/10.1021/es0158861>.
- H. Ritchie and M. Rosr. CO₂ and Greenhouse Gas Emissions, 5 2020. URL <https://ourworldindata.org/co2-and-other-greenhouse-gas-emissions><https://ourworldindata.org/emissions-by-sector><https://ourworldindata.org/co2-and-other-greenhouse-gas-emissions%0Ahttps://ourworldindata.org/emissions-by-sector>.
- J. Sarkar and S. Bhattacharyya. Application of graphene and graphene-based materials in clean energy-related devices Minghui. *Archives of Thermodynamics*, 33(4):23–40, 2012. ISSN 12310956. doi: 10.1002/er.
- G. Sartori. PROCESS FOR REMOVING CARBON DOXDE CONTAINING ACIDIC GASES FROM GASEOUS MIXTURES USING AQUEOUS AMNE SCRUBBENG SOLUTIONS, 1978.
- W. Schakel, C. R. Hung, L. A. Tokheim, A. H. Strømman, E. Worrell, and A. Ramírez. Impact of fuel selection on the environmental performance of post-combustion calcium looping applied to a cement plant. *Applied Energy*, 210:75–87, 1 2018. ISSN 03062619. doi: 10.1016/j.apenergy.2017.10.123.
- C. Song, Q. Liu, S. Deng, H. Li, and Y. Kitamura. Cryogenic-based CO₂ capture technologies: State-of-the-art developments and current challenges, 3 2019. ISSN 18790690.
- J. G. Speight. Hydrogen Production. *Heavy Oil Recovery and Upgrading*, pages 657–697, 2019. doi: 10.1016/B978-0-12-813025-4.00015-5. URL <https://linkinghub.elsevier.com/retrieve/pii/B9780128130254000155>.

- I. S. Pieta, A. Lewalska-Graczyk, P. Kowalik, K. Antoniak-Jurak, M. Krysa, A. Sroka-Bartnicka, A. Gajek, W. Lisowski, D. Mrdenovic, P. Pieta, R. Nowakowski, A. Lew, and E. M. Serwicka. Co₂ hydrogenation to methane over ni-catalysts: The effect of support and vanadia promoting. *Catalysts*, 11(4), 4 2021. ISSN 20734344. doi: 10.3390/catal11040433.
- Statista. Cement production worldwide, 2020. URL [https://www.statista.com/statistics/373845/global-cement-production-forecast/](https://www.statista.com/statistics/373845/global-cement-production-forecast/?fbclid=IwAR13xM7qTnRyScAWr95Rd60qiPHATvg2q9xF15GUKu0bCA4eXjN2q4qPQV0https://www.statista.com/statistics/373845/global-cement-production-forecast/).
- S. Sutanto, J. W. Dijkstra, J. A. Pieterse, J. Boon, P. Hauwert, and D. W. Brilman. CO₂ removal from biogas with supported amine sorbents: First technical evaluation based on experimental data. *Separation and Purification Technology*, 184:12–25, 2017. ISSN 18733794. doi: 10.1016/j.seppur.2017.04.030. URL [https://reader.elsevier.com/reader/sd/pii/S138358661731256X?token=389A28E90EC0B9B](https://reader.elsevier.com/reader/sd/pii/S138358661731256X?token=389A28E90EC0B9B282E666E6DA523BEA4E30F190177403576D4E4F38DB3B19AAE2913615E5D405C532939590D9EDDAA8&originRegionhttps://reader.elsevier.com/reader/sd/pii/S138358661731256X?token=389A28E90EC0B9B).
- M. Svarer. Grøn skattereform - Første delrapport. Technical report, Ekspertgruppen for en Grøn skattereform, 2022.
- W. Tong, M. Forster, F. Dionigi, S. Dresp, R. Sadeghi Erami, P. Strasser, A. J. Cowan, and P. Farràs. Electrolysis of low-grade and saline surface water, 5 2020. ISSN 20587546.
- M. V. Twigg and M. S. Spencer. Deactivation of copper metal catalysts for methanol decomposition, methanol steam reforming and methanol synthesis. *Topics in Catalysis*, 22(3-4):191–203, 4 2003. ISSN 10225528. doi: 10.1023/A:1023567718303. URL <https://link.springer.com/article/10.1023/A:1023567718303>.
- . UNESCO. The United Nations world water development report 2019: leaving no one behind, 2019.

United Nations. Climate Change - United Nations Sustainable Development, 2016.

URL <https://www.un.org/sustainabledevelopment/climate-change/>.

T. Wall. Fundamentals of Oxy-Fuel Combustion, 2005.

L. Wang, Y. Yang, W. Shen, X. Kong, P. Li, J. Yu, and A. E. Rodrigues. CO₂ capture from flue gas in an existing coal-fired power plant by two successive pilot-scale VPSA units. *Industrial and Engineering Chemistry Research*, 52(23):7947–7955, 2013. ISSN 08885885. doi: 10.1021/ie4009716. URL <https://pubs.acs.org/sharingguidelines>.

Appendix A

Sub-Blocks in CCC Model

In this appendix, the two sub-blocks from Figure 4.1 are described and elaborated. Firstly, the dryer is presented, which is based on several flash stages and a water knock out. Subsequently, the contact liquid refrigerant circuit is presented.

A.1 Dryer Component

The sub-block called "DRYERCOM" in Figure 4.1, from Chapter 4 covers the equipment illustrated in Figure A.1. The dryer component has to remove the water content in the off-gas prior to the desublimation column to prevent ice formation. The process is based on a cascade flash separation with a separator in the end to ensure a total water knockout.

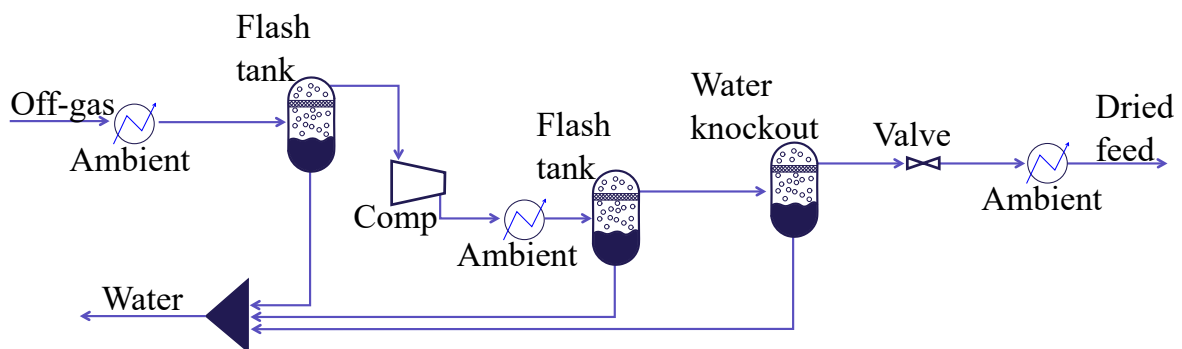


Figure A.1: Schematic overview of the drying process prior to the CCC model.

Initially, the off-gas is cooled to 5 °C by either heat exchanging with the ambient air or seawater. Subsequently, the off-gas enters the first flash tank, which separates the water from the off-gas. The off-gas from the first flash tank is pressurised to 3.21 bar, which is equivalent to a maximum pressure ratio of 3. After the pressurisation, the off-gas is cooled to 10 °C prior to the second flash tank. After the second flash tank, the water content is sufficiently low to be neglected in the CCC model. Therefore, a separator is included to ensure a total water knockout before the off-gas is injected into the desublimation column. Finally, the off-gas is passed through a valve and a heat exchanger in order to reduce the pressure and temperature to 1.07 bar and 5 °C, respectively.

A.2 Contact Liquid Coolant Circuit

The other sub-block "CLCOOL" presented in Figure 4.1 covers the refrigerant circuit cooling the contact liquid before entering the desublimation column. The equipment included in the contact liquid refrigerant circuit is presented in Figure A.2.

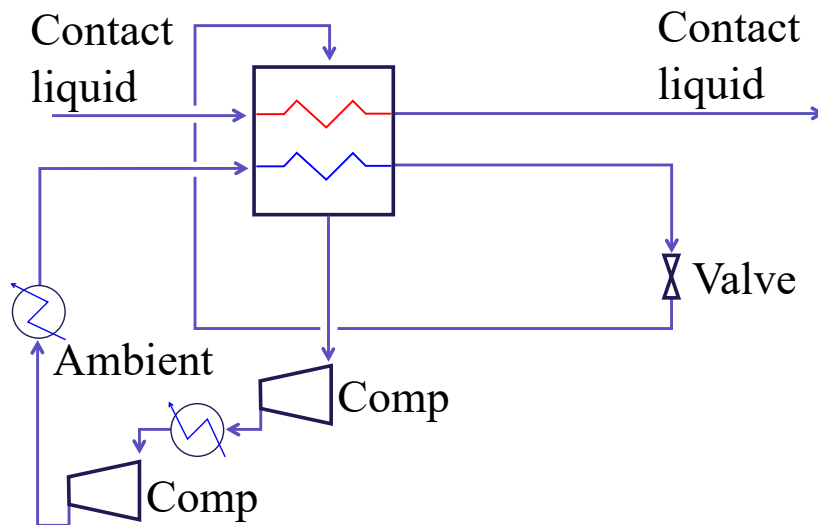


Figure A.2: Schematic overview of the contact liquid refrigerant circuit.

The refrigerant circuit aims to cool the contact liquid to -125 °C prior to the desublimation column. In order to obtain the desired temperature, the contact liquid heat

exchanges with a refrigerant circuit in a multi-stream heat exchanger. The refrigerant circuit is a closed-loop including a cascade compression and heat exchanging. During the cascade compression and heat exchange, the refrigerant obtains a pressure of 36.95 bar and a temperature of 31.85 °C before it enters the multi-stream heat exchanger. In the multi-stream heat exchanger, the refrigerant is further cooling, before it enters a valve to obtain the inlet temperature of -166.45 °C. During the multi-stream heat exchanger, the refrigerant is heated to 13.25 °C by heat exchanging with itself and the contact liquid. The mass flow required to cool the contact liquid from 15 °C to -125 °C is determined to 173,915 kg/hour.

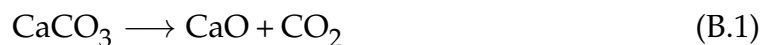
Appendix B

Mass Flow Calculation of the combustion and utilisation processes

In this appendix, the mass flow calculations from sections 5 and 2.1.1 are elaborated. The mass flow rates are calculated based on balancing the reactions with the corresponding molar masses of the compounds.

B.1 Specification of the Mass Flows for the Combustion Process

The annual CaCO_3 consumption used at Aalborg Portland in 2019 is used to estimate the mass flow rate of the fuel and oxidiser required for the combustion process (Aalborg Portland A/S, 2019a). Firstly, the calcination enthalpy of the reaction is determined. The calcination reaction is presented in equation (B.1).



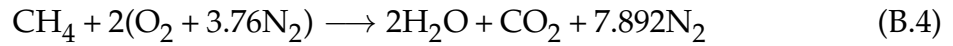
The standard enthalpy of reaction is calculated based on the sum of standard enthalpies for the products subtracted from the sum of the standard enthalpy of the reactants, as presented in equation (B.2).

$$\Delta H_{\text{reaction}}^0 = (\Delta H_{\text{CaO}}^0 + \Delta H_{\text{CO}_2}^0) - \Delta H_{\text{CaCO}_3}^0 \quad (\text{B.2})$$

Based on the calcination reaction and the standard enthalpies, the calcination enthalpy of the reaction can be calculated to 178 kJ/mol-CaCO₃. Additionally, the energy consumption to cover the preheating of limestone and dissociation has been estimated to be 159 kJ/mol-CaCO₃ based on the Aspen Plus[®] model. Furthermore, a heat loss to the surrounding of 50.51 kJ/mol-CaCO₃ is likewise considered. Combined the total energy consumption for the calcination process is expected to be 387.64 kJ/mol-CaCO₃. As a result, the corresponding mass flow rate of fuel required to force the calcination process can be calculated. The fuel flow rate can be calculated, based on equation (B.3).

$$\dot{m}_{\text{fuel}} = \frac{\dot{Q}_{\text{tot,cal}}}{LHV_{\text{fuel}}} \quad (\text{B.3})$$

$\dot{Q}_{\text{tot,cal}}$ from equation (B.3) is the total energy consumption from the calcination multiplied by the annual molar flow of CaCO₃ based on data from Aalborg Portland A/S (2019a). Furthermore, the corresponding air supply to obtain stoichiometric combustion can be calculated based on the fuel consumption. The air required for the combustion can be determined based on the fuel specified Air to Fuel ratio (AFR). The AFR is the ratio between air and fuel to obtain a stoichiometric combustion. Thus, the AFR is based on the combustion reaction and the molar masses of the fuel and air. The balanced methane combustion reaction is presented in equation (B.4).



Subsequently, the molar masses of the methane and air in the reaction is determined in equation (B.5) and (B.6) respectively.

$$1 \text{ mol} \cdot 16 \text{ g/mol} = 16 \text{ g} \quad (\text{B.5})$$

$$2 \text{ mol} \cdot (32 \text{ g/mol} + 3.76 \cdot 28 \text{ g/mol}) = 274.56 \text{ g} \quad (\text{B.6})$$

Finally, the AFR can be determined as presented in equation (B.7).

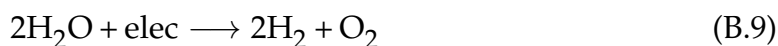
$$\text{AFR} = \frac{m_{\text{air}}}{m_{\text{fuel}}} = \frac{274.56 \text{ g}}{16 \text{ g}} = 17.16 \quad (\text{B.7})$$

In accordance with equation (B.7), the mass flow of air to obtain stoichiometric methane combustion can be specified. However, if oxyfuel combustion is used,

the AFR will be recalculated, as the nitrogen from equation (B.4) will disappear. Consequently, the AFR for oxyfuel combustion will be 3.9969.

B.2 Scaling Specifications for the Utilisation Facility and the Electrolysis Process

In order to calculate the resulting hydrogen production required to make a conversion of all the captured CO₂, the following reactions are considered. It appears from equation (B.8), that the methanation requires 4 moles of hydrogen per mole of CO₂ to start the reaction. The hydrogen production is expected to come from an alkaline electrolysis process, which is presented in equation (B.9).



Based on the reactions, the molar masses of the compounds, and the knowledge about the CO₂ mass flow from the CCC model, the corresponding mass flows for the remaining components can be determined. The molar masses for the different components are stated in Table B.1.

Table B.1: Molar mass of the compounds in reaction (B.8), and (B.9).

Compound	Molar mass [g/mol]
CO ₂	44
Methane	16
Water	18
Oxygen	16
Hydrogen	2

Based on the CCC process modelled in Aspen Plus[®], the annual molar flow of CO₂ is estimated to 4.88·10⁷ kmole/year. This annual CO₂ capture forms the basis to determine the corresponding mass flows of the other components, based on equation (B.8) and (B.9). The resulting mass flows are presented in Table B.2.

Table B.2: Calculated mass flow rates of the compounds based on molar masses and reactions.

Compound	Mass flow rate [tonne/year]
CO ₂	2.15·10 ⁶
Oxygen	3.12·10 ⁶
Hydrogen	393,172
Water	3.51·10 ⁶
Methane	782,232